# Ice nucleating particles at a coastal marine boundary layer site: correlations with aerosol type and meteorological conditions

**Authors:** R. H. Mason[1], M. Si[1], J. Li[2], C. Chou[1], R. Dickie[1], D. Toom-Sauntry[3], C. Pöhlker[4], J. D. Yakobi-Hancock[5], L. A. Ladino[5], K. Jones[6], W. R. Leaitch[3], C. L. Schiller[6], J. P. D. Abbatt[5], J. A. Huffman[2*], A. K. Bertram[1*]

**Affiliations:**

[1]Department of Chemistry, University of British Columbia, Vancouver, BC, V6T1Z1, Canada

[2]Department of Chemistry and Biochemistry, University of Denver, Denver, CO, 80208, USA

[3]Climate Research Division, Environment Canada, Toronto, ON, M3H5T4, Canada

[4]Biogeochemistry Department, Max Planck Institute of Chemistry, Mainz, 55020, Germany

[5]Department of Chemistry, University of Toronto, Toronto, ON, M5S3H6, Canada

[6]Air Quality Science Unit, Environment Canada, Vancouver, BC, V6C3S5, Canada

[*]Correspondence to: bertram@chem.ubc.ca (A. K. Bertram), alex.huffman@du.edu (J. A. Huffman)

**Abstract:**

Information on what aerosol particle types are the major sources of ice nucleating particles (INPs) in the atmosphere is needed for climate predictions. To determine which aerosol particles are the major sources of immersion-mode INPs at a coastal site in Western Canada, we investigated correlations between INP number concentrations and both concentrations of different atmospheric particles and meteorological conditions. We show that INP number concentrations are strongly correlated with the number concentrations of fluorescent bioparticles between -15 and -25 °C, and that the size distribution of INPs is most consistent with the size distribution of fluorescent bioparticles. We conclude that biological particles were likely the major source of ice nuclei at freezing temperatures between -15 and -25 °C at this site for the time period studied. At -30 °C, INP number concentrations are also well correlated with number concentrations of the total aerosol particles ≥ 0.5 μm, suggesting that non-biological particles may have an important contribution to the population of INPs active at this temperature. As we found that black carbon particles were unlikely to be a major source of ice nuclei during this study, these non-biological INPs may include mineral dust. Furthermore, correlations involving chemical tracers of marine aerosols and marine biological activity, sodium and methanesulfonic acid, indicate that the majority of INPs measured at the coastal site likely originated from terrestrial rather than marine sources. Finally, six existing empirical parameterizations of ice nucleation were tested to determine if they accurately predict the measured INP number concentrations. We found that none of the parameterizations selected are capable of predicting INP number concentrations with high accuracy over the entire temperature range investigated. This finding illustrates that additional measurements are needed to improve parameterizations of INPs and their subsequent climatic impacts.

## 1. Introduction

The formation of ice in the atmosphere can occur by two primary mechanisms: homogeneous and heterogeneous ice nucleation. Homogeneous nucleation can only occur at temperatures below approximately -37 °C. However, heterogeneous nucleation can occur at all temperatures below 0 °C. In the atmosphere, heterogeneous nucleation occurs on solid or partially solid aerosol particles termed ice nucleating particles (INPs). INPs are a small subset of the total aerosol population (Rogers et al., 1998) whose unique surface properties make them capable of lowering the energy barrier to ice nucleation and hence cause freezing at warmer temperatures or lower supersaturations with respect to ice compared to homogeneous nucleation. Four modes of nucleation have been identified (Vali, 1985; Vali et al., 2015): deposition nucleation where ice forms on the INP directly from the gas phase; condensation freezing where ice forms during the condensation of water onto the INP; immersion freezing where ice forms on an INP within a supercooled droplet; and contact freezing where the impact of a supercooled droplet by an INP initiates freezing. In this study we focus on immersion freezing, which is relevant to ice formation in mixed-phase clouds.

The presence of INPs in the atmosphere can lead to changes in the microphysical properties and lifetime of clouds. As a result, a change in INP concentrations can indirectly modify climate by changing cloud optical properties, lifetime, and cloud extent (e.g. Baker, 1997; Lohmann, 2002; Storelvmo et al., 2011; Creamean et al., 2013). Currently, the role of INPs in climate change is highly uncertain (Boucher et al., 2013). To predict the role of INPs in climate change and precipitation, information on what particle types are the major sources of INPs in the atmosphere is needed. Possible candidates for INPs in the atmosphere include mineral dust, primary biological particles, and black carbon (BC). Primary biological INPs are

65 believed to be dominant above -15 °C while below this temperature non-biological INPs may be
66 of greater importance (Murray et al., 2012).

67 Mineral dust particles have long been known to be efficient INPs (Mason and Maybank,
68 1958). Numerous laboratory studies have found that different types of mineral dust particles can
69 effectively nucleate ice in both the immersion and deposition modes; for example kaolinite
70 (Lüönd et al., 2010; Wheeler and Bertram, 2012), Arizona test dust (Kanji and Abbatt, 2010;
71 Knopf and Koop, 2006; Marcolli et al., 2007; Niedermeier et al., 2010), NX illite (Broadley et
72 al., 2012), natural Asian and Saharan dust samples (Field et al., 2006; Kulkarni, 2010), and more
73 recently feldspar (Atkinson et al., 2013; Yakobi-Hancock et al., 2013). Both field studies
74 (DeMott et al., 2003; Cziczo et al., 2004; Richardson et al., 2007; Klein et al., 2010; Chou et al.,
75 2011; Creamean et al., 2013) and modeling studies (Hoose et al., 2010b) also suggest that
76 mineral dust can be a dominant INP in the atmosphere.

77 Primary biological particles have also been identified as a possible source of INPs (e.g.
78 Szyrmer and Zawadzki, 1997; Möhler et al., 2007; Garcia et al., 2012; Hiranuma et al., 2015).
79 The ocean and continents are both potential sources of ice-active primary biological particles
80 (Hoose and Möhler, 2012; Murray et al., 2012). Model studies have shown that biological
81 particles may not be important for ice nucleation on a global and annual scale (Hoose et al.,
82 2010; Sesartic et al., 2013; Spracklen and Heald, 2014), but may be important on regional and
83 seasonal scales, especially if concentrations of biological particles are high or concentrations of
84 other types of INPs are low (Phillips et al., 2009; Sun et al., 2012; Burrows et al., 2013;
85 Creamean et al., 2013; Yun and Penner, 2013; Costa et al., 2014; Spracklen and Heald, 2014).

86 Ice-active biological particles from continental sources include bacteria (e.g. Maki et al.,
87 1974; Lindow et al., 1978; Maki and Willoughby, 1978; Kozloff et al., 1983), fungal spores (e.g.

88 Jayaweera and Flanagan, 1982; Tsumuki et al., 1992; Richard et al., 1996; Iannone et al., 2011;
89 Haga et al., 2013; Morris et al., 2013), and pollen (e.g. Diehl et al., 2001, 2002; von Blohn et al.,
90 2005; Pummer et al., 2012; Augustin et al., 2013; Hader et al., 2014; O Sullivan et al., 2015). In
91 addition, strong correlations between number concentrations of INPs and primary biological
92 particles have been found during studies in the Amazon and United States in forested regions
93 (Prenni et al., 2009b, 2013; Huffman et al., 2013; Tobo et al., 2013), and biological particles
94 have been observed in ice-crystal residuals of mixed-phase clouds (e.g. Pratt et al., 2009), cloud
95 water (e.g. Joly et al., 2014), and snow samples (e.g. Christner et al., 2008; Morris et al., 2008;
96 Hill et al., 2014). Ice-active biological particles have also been associated with soils (Conen et
97 al., 2011; O'Sullivan et al., 2014; Tobo et al., 2014; Fröhlich-Nowoisky et al., 2015).

98 Biological material found in the ocean that may be a source of INP in the atmosphere
99 includephytoplankton, bacteria, and biological material in the sea surface microlayer. Studies
100 have indicated bacteria and phytoplankton found in seawater and sea ice are a potential source of
101 INP in the atmosphere (Schnell, 1975, 1977; Schnell and Vali, 1975; Jayaweera and Flanagan,
102 1982; Parker et al., 1985; Alpert et al., 2011; Knopf et al., 2011). Material in the sea surface
103 microlayer has also been found to exhibit ice-activity (Wilson et al., 2015), and previous work
104 has indicated that biological material generated during phytoplankton blooms may be a source of
105 INPs in the atmosphere (Prather et al., 2013; DeMott et al., 2015). The modeling work of
106 Burrows et al. (2013) indicates that ice-active primary biological particles from the ocean may be
107 particularly important in remote regions such as the Southern Ocean.

108 Another potential type of INP in the atmosphere is BC (Kärcher et al., 2007). Laboratory
109 studies have given varying results on whether BC particles act as efficient INPs under
110 atmospherically-relevant conditions (e.g. Gorbunov et al., 2001; Möhler et al., 2005; Dymarska

et al., 2006; Kärcher et al., 2007; DeMott et al., 2009; Friedman et al., 2011; Cziczo et al., 2013; Brooks et al., 2014), although BC is generally considered to be less efficient than mineral dust in the immersion mode (Hoose and Möhler, 2012; Murray et al., 2012; and references therein). Field studies have also produced varying results (e.g. Lin et al., 2006; Cozic et al., 2008; Kamphus et al., 2010; Twohy et al., 2010; Ebert et al., 2011; Corbin et al., 2012; Cziczo et al., 2013; Knopf et al., 2014; McCluskey et al., 2014). Models have suggested that carbonaceous aerosols may have a significant indirect effect on climate if they efficiently nucleate ice (e.g. Lohmann, 2002; Liu et al., 2009; Penner et al., 2009; Yun and Penner, 2013).

To determine which aerosol particles are the major source of INPs in the immersion mode at a coastal site in Western Canada, we investigate correlations between INP number concentrations and both concentrations of different atmospheric particle types and meteorological conditions. Measurements were conducted in August 2013 as part of the NETwork on Climate and Aerosols: addressing key uncertainties in Remote Canadian Environments (NETCARE) project (http://netcare-project.ca/). A primary goal of the study was to investigate whether primary biological particles and BC particles are a major source of INPs at this site and determine if the ocean contributes to the measured INP population at this coastal site. In addition, we also test the ability of parameterizations reported in the literature at predicting the INP number concentrations measured at this coastal site.

## 2. Methods

### 2.1 Site description and instrument location

Measurements were performed at Amphitrite Point (48.92° N, 125.54° W) on the west coast of Vancouver Island in British Columbia, Canada. This was also the location of studies on ozone (McKendry et al., 2014) and cloud condensation nuclei (Yakobi-Hancock et al., 2014).

Amphitrite Point (Fig. 1) is located approximately 2.2 km south of the town of Ucluelet (population of 1627 in 2011; Statistics Canada, 2012). The largest nearby population centers are Nanaimo 120 km to the east, Victoria 170 km to the southeast, and Vancouver 180 km to the east. This region has a temperate maritime climate, characterized by warm summers, mild winters, and relatively high levels of cloud cover and precipitation. According to the Köppen-Geiger classification scheme (Kottek et al., 2006), the climate type is Cfb which denotes a mild mid-latitude and moist climate (C) with no dry season (f), and a moderate summer where the average hottest-month temperature is < 22 ºC and at least four months have an average temperature > 10 ºC (b). Local forests contain predominantly coniferous tree species including western hemlock, western redcedar, and Douglas-fir that is characteristic of most low-elevation sites along the west coast of Canada (Austin et al., 2008). The Pacific Ocean is west and south of the site, where the mixing of iron-rich coastal waters with nitrate-rich oceanic waters produces a zone of high primary productivity (Whitney et al., 2005; Ribalet et al., 2010). Measurements were carried out from August 6–27, 2013. Specifics on the sampling times (i.e. start and end times) are given in Table S1 of the Supplement.

Aerosol instrumentation was located in one of two mobile laboratories; one specific to the NETCARE project (labeled 1 in Fig. 1) and one operated by Environment Canada, the British Columbia Ministry of Environment, and Metro Vancouver (labeled 2 in Fig. 1). Aerosols were sampled through louvered total suspended particulate inlets (Mesa Labs Inc., Butler, NJ, USA) or louvered $PM_{10}$ inlets (Thermo Scientific, Waltham, MA, USA) atop masts extending 5.5 m agl. The two mobile laboratories were approximately 20 m above mean sea level and 100 m from the high tide line of the Pacific Ocean (McKendry et al., 2014). A row of trees and shrubs approximately 2–10 m in height stood between the laboratories and the rocky shoreline.

157 Adjacent to the laboratories on their seaward side was Amphitrite Lighthouse (labeled 3 in Fig.
158 1) and Wild Pacific Trail, local tourist attractions and a source of foot traffic during fair weather.
159 Immediately north and east of the site was a station of the Canadian Coast Guard (labeled 4 in
160 Fig. 1).

161 The majority of the meteorological parameters reported in this study were measured at
162 Amphitrite Lighthouse, located approximately halfway between the mobile laboratories and the
163 ocean. Relative humidity and temperature were monitored using an HMP45C probe (Campbell
164 Scientific, Logan, UT, USA) with accuracies of ± 3 % and ± 0.2 °C, respectively. Wind direction
165 and wind speed were determined by a model 05305L Wind Monitor (R. M. Young, Traverse
166 City, Michigan, USA) to a respective accuracy of ± 3° and ± 0.2 m $s^{-1}$. Measurements of wind
167 speed were also obtained from a moored buoy located in La Perouse Bank, approximately 35 km
168 to the WSW of the Amphitrite Point sampling site (station 46206; 48.84° N, 126.00 °W;
169 National Data Buoy Center, 2013). The cup anemometer used to measure wind speed on the
170 buoy was positioned at 5 m asl.

171 **2.2 Ice nucleating particle measurements**

172 INP number concentrations in the immersion mode were determined using the micro-
173 orifice uniform deposit impactor-droplet freezing technique (MOUDI-DFT; Mason et al., 2015).
174 A Model II 120R MOUDI (MSP Corp., Shoreview, MN, USA) collected size-fractionated
175 aerosol samples by inertial separation (Marple et al., 1991) onto hydrophobic glass cover slips
176 (HR3-215; Hampton Research, Aliso Viejo, CA, USA). To compensate for the thickness of the
177 hydrophobic glass cover slips, spacers were placed between the MOUDI stages. Custom
178 substrate holders were added to the MOUDI impaction plates to maintain consistent positioning
179 of the hydrophobic glass cover slips within the impactor (Mason et al., 2015). Samples from

MOUDI stages 2–8 were used in this study, corresponding to a particle size range of 10–0.18 μm (50 % cutoff aerodynamic diameter). Thirty-four sets of MOUDI samples were collected; 18 during the day and 16 at night. The average collection time of a MOUDI sample was 7.8 hours. Details of each INP sampling period are available in Table S1 of the Supplement.

The ice-nucleating ability of particles collected by the MOUDI was then determined by the droplet freezing technique (DFT; Koop et al., 2000; Iannone et al., 2011; Mason et al., 2015; Wheeler et al., 2015). Within 24 hours of collection, samples were placed in a temperature- and humidity-controlled flow cell that was coupled to an optical microscope (Axiolab; Zeiss, Oberkochen, Germany) with a 5× magnification objective. At a sample temperature of 0 °C a humidified gas flow was introduced, resulting in the formation of water droplets on the sample. Following droplet growth by condensation and coalescence, the droplet size was decreased with a dry gas flow to a final size of approximately 80–160 μm in diameter. On average, more than 99 % of particles on the surface of the hydrophobic glass cover slip were incorporated into droplets by this procedure. Closing valves upstream and downstream of the cell then isolated the flow cell, and the sample temperature was lowered at a constant rate of -10 °C $min^{-1}$ to -40 °C. This cooling rate was chosen to minimize the freezing of a liquid droplet by contact with a growing ice crystal. Recent work suggests that changing the cooling rate by an order of magnitude may lead to a shift in freezing temperatures of approximately 0.5–2 °C (Murray et al., 2011; Broadley et al., 2012; Welti et al., 2012; Wright and Petters, 2013; Wright et al., 2013; Wheeler et al., 2015). During droplet growth, evaporation, and cooling, a CCD camera connected to the optical microscope recorded a digital video of the sample. Using the video timestamp and a resistance temperature detector positioned within the flow cell, which was calibrated against the melting point of water droplets approximately 100 μm in diameter, the freezing temperature of each

droplet was found by manually noting the increase in droplet opacity immediately following ice nucleation.

Since a small fraction of the sampled particles (less than 1 % on average) was not included in the droplets, there was the possibility of deposition nucleation as well. However, based on an analysis of the videos recorded during the ice nucleation experiments, fewer than 3 % of all freezing events observed were the result of deposition nucleation. Due to the low occurrence of deposition nucleation, only immersion freezing results are reported.

The atmospheric number concentration of INPs within the size cut of each MOUDI stage, [INPs($T$)], was evaluated using the following equation:

$$[\mathrm{INPs}(T)] = -\ln\left(\frac{N_\mathrm{u}(T)}{N_\mathrm{o}}\right) N_\mathrm{o} \left(\frac{A_\mathrm{deposit}}{A_\mathrm{DFT} V}\right) f_\mathrm{nu} f_\mathrm{ne} \qquad (1)$$

where $N_\mathrm{u}(T)$ is the number of unfrozen droplets at temperature $T$, $N_\mathrm{o}$ is the total number of droplets, $A_\mathrm{deposit}$ is the total area of the sample deposit on the hydrophobic glass cover slips, $A_\mathrm{DFT}$ is the area of the sample analyzed by the DFT, $V$ is the volume of air sampled by the MOUDI, $f_\mathrm{nu}$ is a correction factor to account for changes in particle concentration across each MOUDI sample (because the DFT analyzes only a fraction of the entire sample), and $f_\mathrm{ne}$ is a correction factor to account for the uncertainty associated with the number of nucleation events in each experiment following Koop et al. (1997). Additional details are available in Mason et al. (2015). Equation (1) takes into account the possibility of multiple INPs being contained in a single droplet using the method of Vali (1971). The total INP number concentration was found by summing the INP number concentrations over all analyzed MOUDI stages. Here we report INP data between -15 and -30 °C as few (1.3 %) of droplets froze at temperatures > -15 °C, and in some experiments all droplets were frozen at temperatures < -30 °C, which prohibited the

calculation of INP number concentrations by Eq. (1). INP number concentrations have been adjusted to standard temperature and pressure.

### 2.3 Total and fluorescent aerosol measurements with sizes ≥ 0.5 μm

A model-4A waveband integrated bioaerosol sensor (WIBS-4A; Droplet Measurement Technologies, Boulder, CO, USA) was used to find both the total and fluorescent aerosol number concentrations with sizes ≥ 0.5 μm. Particles that enter the WIBS-4A first transect a continuous-wave 635 nm diode laser. The forward-scattered light from the continuous-wave laser is detected with a quadrant photomultiplier tube for the determination of particle size and asymmetry factor based on the signal intensity and asymmetry, respectively. The detected forward-scattered light also triggers excitation pulses from xenon lamps, the first at a wavelength of 280 nm and the second at 370 nm. The excitation pulses may lead to fluorescent emission from the particle, which is then collected in two wavelength ranges: 310–400 nm (short wavelength region) and 420–650 nm (long wavelength region). This results in sample information provided for each particle in three fluorescence channels: excitation at 280 nm, emission in the short wavelength region (FL1); excitation at 280 nm, emission in the long wavelength region (FL2); and excitation at 370 nm, emission in the long wavelength region (FL3). Detailed descriptions of the instrument can be found in Kaye et al. (2005), Gabey et al. (2010), and Healy et al. (2012a). The sample and total flow rates of the WIBS-4A were 0.63 and 2.3 L $min^{-1}$, respectively, and number concentrations have been adjusted to standard temperature and pressure.

The fluorescent channels used in the WIBS-4A allow for the detection of fluorophores characteristic of biological activity. These fluorophores include the amino acid tryptophan, the cofactor NAD(P)H, and the micronutrient riboflavin. While some non-biological species such as soot, mineral dusts, polycyclic aromatic hydrocarbons, secondary organic aerosols, and humic-

like substances can produce a fluorescent signal (Pan et al., 1999; Sivaprakasam et al., 2004; Bones et al., 2010; Gabey et al., 2011; Pöhlker et al., 2012; Lee et al., 2013), the number of fluorescent particles is generally considered to be a lower limit to the number of primary biological particles (Huffman et al., 2010, 2012; Pöhlker et al., 2012). In addition, fluorescence microscopy measurements of samples collected during this field study show high concentrations of fluorescent biological particles (see below). Therefore, fluorescent particles detected using the WIBS-4A are hereafter referred to as fluorescent bioparticles.

Although the WIBS was used to determine the total and fluorescent aerosol number concentrations with sizes ≥ 0.5 μm, it should be noted that the counting efficiency of the WIBS for polystyrene latex spheres with particle diameters of 0.5 μm is roughly 50 % (Healy et al., 2012b). Hence**,** concentration of particles reported here in the 0.5–1 μm size range should be considered as lower limits.

### 2.4 Fluorescence microscopy

Aerosol samples were collected onto glass cover slips using a custom single-stage impactor operating at a flow rate of 1.2 L $min^{-1}$ with a 50 % cutoff aerodynamic diameter of 0.5 μm. Prior to sample collection, the substrates were coated with a thin layer of high viscosity grease (Baysilone grease, Bayer, Germany) to reduce particle bounce.

Fluorescence microscopy images were taken on a BZ-9000 fluorescence microscope (Keyence, Inc., Osaka, Japan) equipped with a 120 W super high-compression mercury lamp and a 1.5 megapixel monochrome CCD camera. Images were obtained using the following fluorescence filters: OP-66834 DAPI-BP ($\lambda_{ex}$ = 360/20 nm, $\lambda_{dichroic}$ = 400 nm, $\lambda_{abs}$ = 460/25 nm), OP-66836 GFP-BP ($\lambda_{ex}$ = 470/20 nm, $\lambda_{dichroic}$ = 495 nm, $\lambda_{abs}$ = 535/25 nm), and OP-66838 TexasRed ($\lambda_{ex}$ = 560/20 nm, $\lambda_{dichroic}$ = 595 nm, $\lambda_{abs}$ = 630/30 nm). Filter specifications are given

as wavelength of maximum absorbance or excitation and full width at half maximum (λ/FWHM).

### 2.5 Black carbon (BC) measurements

BC mass concentrations were measured using a multi-angle absorption photometer (MAAP model 5012; Thermo Scientific, Franklin, MA, USA). Detailed descriptions of the MAAP are available in Petzold et al. (2002), Petzold and Schönlinner (2004), and Petzold et al. (2005). Within the MAAP, particles are continuously collected on a glass fiber filter. The intensity of transmitted and forward-scattered light through the aerosol particle layer and filter matrix is measured by a photodetector located beneath the filter at a frequency of 1 Hz. The signal strength is attenuated by the presence of both light-absorbing particles and particles that cause backscattering. As the angular distribution of back-scattered light is related to the fraction of non-absorbing particles (Petzold and Schönlinner, 2004), four additional photodetectors located above the filter are used to quantify the non-absorbing component of the sample. The absorbance by the collected aerosol is then related to a mass of BC using a mass-specific absorption coefficient of 6.6 $m^2 g^{-1}$. Mass concentrations have been adjusted to standard temperature and pressure.

Non-BC material such as mineral dusts and brown carbon can also absorb 670 nm wavelength light used in the MAAP, albeit with smaller absorption coefficients than BC (Yang et al., 2009). We follow the recommendation of Petzold et al. (2013) for BC data derived from optical absorption methods and hereafter refer to MAAP data as measurements of equivalent black carbon (eBC).

### 2.6 Tracers of anthropogenic aerosols

Measurements of CO, $NO_x$, and $SO_2$ were used to identify anthropogenic contributions to the sampled air masses as sources of these gases include fossil fuel combustion and biomass burning (Galanter et al., 2000; Gadi et al., 2003; United States Environmental Protection Agency, 2014). CO concentrations were monitored using a Thermo Fisher Scientific 48i-TL, an absorbance-based analyzer using infrared light at a wavelength of 4.6 μm. $NO_x$ concentrations were monitored using chemiluminescence with a Thermo Fisher Scientific 42i. This instrument first converts $NO_2$ to NO, which then reacts with ozone to produce luminescence of intensity in proportion to the level of $NO_x$. A Teledyne API T100U, using fluorescence emitted by $SO_2$ under excitation by ultraviolet light, monitored $SO_2$ concentrations. Data were collected for each instrument at a frequency of 1 $min^{-1}$.

### 2.7 Ion measurements

Size-resolved aerosol samples were collected on Teflon® filters (Pall Corporation, Port Washington, NY, USA) using a second MOUDI (model 110R). Samples were collected on the inlet, stage 1, and stages 7–10 of the MOUDI with stages 2–6 being removed prior to collection. The flow rate through the MOUDI was on average 24 L $min^{-1}$, resulting in a collected size range of 0.068 μm to > 20 μm (50 % cutoff aerodynamic diameter). Collection times ranged from approximately 45–49 hours and samples were stored at 4 °C for a period of one month before analysis.

Mass concentrations of sodium and methanesulfonic acid (MSA) were found using cationic and anionic chromatography following the method of Phinney et al. (2006). Briefly, filters were extracted with sonication in 10 mL of deionized water for 1 hour, and samples were analyzed with a Dionex DX600 ion chromatograph using an AS11-HC column and a CS12 column for anions and cations, respectively. Filter blanks were measured to be below the limit of

316 detection for both analytes. Mass concentrations were adjusted to standard temperature and
317 pressure.

318 **2.8 Back trajectories**

319 Back trajectories spanning a period of 72 hours were calculated for each sampling period
320 using the Hybrid Single-Particle Lagrangian Integrated Trajectory (HYSPLIT4) model of the
321 National Oceanographic and Atmospheric Administration and the GDAS1 meteorological data
322 archive (Draxler and Rolph, 2014). To determine if the air mass changed during a sampling
323 period, back trajectories were initiated at the beginning of the sampling period and every 2 hours
324 until the end of the sampling period. Back trajectories were used to assign each sampling period
325 to one of four general air mass categories: (i) *coastal NW* where boundary layer air (defined here
326 as an altitude below 1000 m) has traversed land northwest of the sampling site during its
327 approach; (ii) *coastal SE* where boundary layer air has traversed land southeast of the sampling
328 site during its approach; (iii) *Pacific Ocean* where boundary layer air has approached directly
329 from the ocean and has not encountered land prior to arrival at the sampling site; and (iv) *free*
330 *troposphere* where the air mass has spent more than 50 % of the 72 hour back trajectory in the
331 free troposphere. In four sampling periods, back trajectories initiated at different times in the
332 sampling period indicated that the air mass changed during sampling, such as a change in the
333 predominant altitude of the air mass from the free troposphere to the marine boundary layer. In
334 these situations, the air mass category to which the majority of the back trajectories belonged
335 was selected as the air mass category of the sample.

336 **3. Results and discussion**

337 **3.1 Back trajectories and the dependence of INP concentrations on air mass**
338 **classification**

Seventy-two hour back trajectories initiated at the midpoint of each INP sampling period are shown in Fig. 2. The back trajectories indicate that 88 % of the air masses sampled spent the majority of their 72 hours prior to reaching the site over the Pacific Ocean within the marine boundary layer (est. < 1000 m). Furthermore, air masses approached the sampling site from an onshore direction with minimal flow over land apart from coastal regions. Average local wind directions of 89° to 297° during INP sampling support this finding. In Fig. S1 of the Supplement, the back trajectories shown in Fig. 2 are color-coded by the classification of the air mass.

Shown in Fig. 3 is the number concentration of INPs as a function of time, color-coded by the classification of the air mass. There is no obvious trend between INP number concentrations and air mass type at temperatures between -15 and -25 °C. At -30 °C, INP number concentrations associated with air masses from the coastal SE (red points) appear to be higher than INP number concentrations associated with other air masses, but the statistics are low for the coastal SE air masses, especially at -30 °C. Figure 4 shows that the mean values for the different air mass types vary by less than a factor of 2.6. We conclude that INP number concentrations did not exhibit a strong dependence on the type of air mass sampled. The correlation analysis presented in Sects. 3.2–3.5 uses the entire dataset (i.e. the data were not differentiated based on air mass type). We further explore the dependence on air mass type in Sect. 3.6.

### 3.2 Are biological particles a major source of ice nuclei?

To investigate if biological particles are an important source of INPs at the coastal site, we determined correlations between INPs and fluorescent bioparticles. In the following correlation analysis, WIBS-4A data are limited to particle sizes of 10 μm or smaller to better match the size range of the MOUDI-DFT. The correlation coefficients ($R$) of linear fits to the

362 data are presented in Table 1 with correlation plots at a freezing temperature of -25 °C shown in
363 Fig. 5 and plots at -15, -20, and -30 °C given in the Supplement. Here we use the scheme of
364 Dancey and Reidy (2011) where correlations with an *R* value of 0.1–0.3, 0.4–0.6, and 0.7–0.9 are
365 classified as weak, moderate, and strong, respectively. In the discussion, correlations with
366 statistical significance (*P* value < 0.05) are emphasized.

367 With values of *R* between 0.74 and 0.83, INP number concentrations are strongly
368 correlated with the number concentrations of fluorescent bioparticles for INPs active between -
369 15 and -25 °C (Figs. 5a and S3, Table 1). At these temperatures, fluorescent bioparticles have the
370 largest correlation coefficients with INPs compared to all of the other parameters investigated.
371 This suggests that biological particles are an important component of the INP population. Using
372 similar fluorescence techniques, others have also noted strong correlations between INPs and
373 primary biological particles during ambient measurements (Prenni et al., 2009, 2013; Huffman et
374 al., 2013; Tobo et al., 2013).

375 To further investigate the relationship between biological particles and INPs, we
376 compared the size distributions of INPs with the size distributions of total particles and
377 fluorescent bioparticles, using samples where all three measurements were available. Shown in
378 Fig. 6a–d are the average number concentrations of INPs as a function of particle size for droplet
379 freezing temperatures ranging from -15 to -30 °C. The shapes of all four INP size distributions
380 were nearly identical with a single mode at an aerodynamic diameter of 3.2–5.6 μm.

381 Also shown in Fig. 6 are the average size distributions of total particles and fluorescent
382 bioparticles as measured with the WIBS-4A over the size range of 0.5–10 μm. As mentioned in
383 Sect. 2.3, due to the decrease in WIBS counting efficiency at particle sizes below approximately
384 0.7 μm (Healy et al., 2012b), the number concentration of particles sized 0.5–1.0 μm should be

385 considered a lower limit.

386 The size distribution of total particles (Fig. 6e) was found to be unimodal with the mode
387 at 0.5–1.0 μm. Fluorescent bioparticles were bimodally distributed (Fig. 6f) with one mode at
388 1.8–3.2 μm and another at 0.5–1.0 μm. Figure 6 illustrates that the size distributions of INPs are
389 more closely related to the size distribution of fluorescent bioparticles than total particles,
390 suggesting that biological particles may have had a greater contribution to the INP population
391 than non-biological particles.

392 In addition to the WIBS-4A, the presence of biological material in sampled air was
393 verified by fluorescence microscopy. Images of a sample collected on August 11, 2013 are
394 shown in Fig. 7 as an example. The fraction of particles exhibiting fluorescence on this day
395 based on the WIBS-4A was close to the campaign average value; 7.1 % versus an average of 7.8
396 %. The image here shows a sample containing many biological particles, identified by their blue
397 color which is characteristic of biological fluorophores such as proteins and coenzymes (Pöhlker
398 et al., 2012). Most of these biological particles had a similar morphology with an ellipsoidal
399 shape, approximately 11.9 μm in length × 4.1 μm in width, and multi-nucleation with three
400 septa. Morphologically, many of these appear to be fungal macroconidia, consistent with the
401 physical attributes of ascospores (Carlile et al., 2001; Maheshwari, 2005; Leslie and Summerell,
402 2006; Webster and Weber, 2007). Fungal spores can be ice-active at the temperatures used here
403 (Jayaweera and Flanagan, 1982; Pouleur et al., 1992; Tsumuki et al., 1992; Richard et al., 1996;
404 Iannone et al., 2011; Haga et al., 2013, 2014; Fröhlich-Nowoisky et al., 2015), and the size of the
405 bioparticles observed in Fig. 7 (an estimated aerodynamic diameter of 4.8 μm assuming a prolate
406 spheroid shape and unit density) matches the mode in the INP size distributions of Fig. 6.
407 Predicting the optical diameter that the WIBS-4A would measure for such a particle is difficult,

but it is reasonable that they could be detected as slightly larger or smaller depending on the axis upon which the incident light impinges.

### 3.3 Is black carbon a major source of ice nuclei?

Sources of BC at the sampling site include local marine ship traffic. Atmospheric size distributions obtained at other locations demonstrate that most BC particles are smaller than 1 μm (Schwarz et al., 2008, 2013; Schroder et al., 2015). As is shown in Fig. 6, the majority of INPs identified here were larger than 1 μm at all of the temperatures studied. It is therefore likely that BC particles were not the major source of INPs at the sampling site. As correlations between INPs and eBC are moderate at -15 to -25 °C ($R$ = 0.47–0.60, Table 1), we also investigated correlations between INPs and the anthropogenic tracers CO, $NO_x$, and $SO_2$. The correlations between INPs and CO, $NO_x$, and $SO_2$ are not statistically significant (see Table S2 of the Supplement), further suggesting that BC was not a major INP source.

### 3.4 Are particles from the ocean a major source of ice nuclei?

Situated in a region of high oceanic primary productivity (Whitney et al., 2005; Ribalet et al., 2010) with onshore winds, particles of marine origin are a potential source of INPs at the sampling site. Therefore, correlations between INP number concentrations and tracers of marine aerosols and marine biological activity were explored. Since primary marine aerosols are ejected from the ocean by the bursting of entrained bubbles (Blanchard and Woodcock, 1957; Blanchard, 1963, 1989; Andreas, 1998), sodium was used as a tracer of primary particles from the ocean. The strength of correlations between INPs and sodium are given in Table 1. Although the correlations range from weakly-to-moderately negative to strongly positive, the large $P$ values (0.20 or greater) indicate that the results are not statistically significant. Due in part to the long sampling times required for the sodium measurements, only three to six data points were

available for the sodium correlation analysis.

MSA is often used as a marker for marine biological productivity (Saltzman et al., 1986; Savoie et al., 1994; Sorooshian et al., 2009; Gaston et al., 2010; Becagli et al., 2013) because it is chemically stable and its precursor, dimethylsulfide, is produced by primary biological activity in the ocean (Andreae et al., 1985; Charlson et al., 1987; Keller, 1989; Bates et al., 1992; Kettle et al., 1999). As INP number concentrations are closely correlated to bioparticles at warmer droplet freezing temperatures, one may expect correlations of a similar magnitude between INPs and MSA if the marine environment was indeed acting as an important source of biological INPs. As is shown in Table 1, no statistically significant correlations are found as *P* values are large (0.15-0.50).

Finally, correlations between wind speed and INP number concentration were investigated using wind speed data from both the site and an offshore buoy. As the dominant source of bubble entrainment in the oceans is breaking waves (O'Dowd and de Leeuw, 2007), the rate of sea-spray production is dependent in part on wind speed. For this correlation, wind speed was first raised to the power of 3.41 using the power law of Monahan and Muircheartaigh (1980) that relates whitecap coverage to wind speed. The correlations found at -30 °C are statistically significant (*P* value < 0.05), but the magnitude of the correlation coefficients is only moderate (*R* = 0.48–0.55; see Table 1). The average wind speed during INP sampling exceeded the onset speed for whitecap formation, approximately 4 m $s^{-1}$ (O'Dowd and de Leeuw, 2007), in only 47 and 56 % of samples when using the lighthouse and buoy data, respectively, and daily observations at the site noted infrequent wave activity. Furthermore, some of the highest INP concentrations were found when the wind speed was less than 4 m $s^{-1}$. The correlation between local wind direction and INP concentrations was also weak (*R* ranged from -0.19 to -0.32; not

shown).

All correlations between INPs and parameters indicative of marine aerosols and marine biological activity are either moderate at best or not statistically significant. For these reasons, correlations involving sodium, MSA, and wind speed do not provide strong evidence that marine particles were a major contributor to the INP population. Recent measurements have shown the presence of INPs in the sea surface microlayer (Wilson et al., 2015). Our measurements do not contradict these findings since we do not rule out the ocean as a source of INPs. One possibility is that biological INPs released by local vegetation were present in sufficient numbers at this site to overwhelm the presence of any INPs from the ocean.

### 3.5 What is the major source of ice nuclei active at -30 °C?

At warmer droplet freezing temperatures (-15 to -25 °C), the strongest correlations are observed between number concentrations of fluorescent bioparticles and INPs. In contrast, at -30 °C the strength of correlations between INPs and fluorescent bioparticles and INPs and total particles > 0.5 μm in diameter are equal ($R$ = 0.66; Table 1). It is therefore likely that both biological and non-biological particles were important sources of INPs active at -30 °C. Good correlations between INPs and total particles > 0.5 μm have also been observed in several other field studies (e.g. DeMott et al., 2010; Chou et al., 2011; Field et al., 2012; Prenni et al., 2013; Tobo et al., 2013; Jiang et al., 2015).

Since the INP size distributions of Fig. 6 and the correlations of Table 1 do not provide strong evidence of BC particles or the ocean being a major source of INPs active at -30 °C, it is possible that mineral dust was a major source of INPs as mineral dust particles are known to efficiently nucleate ice at this temperature (e.g. DeMott et al., 2003; Cziczo et al., 2004; Field et al., 2006; Möhler et al., 2006; Marcolli et al., 2007; Zimmermann et al., 2008; Klein et al., 2010;

Niedermeier et al., 2010; Chou et al., 2011; Atkinson et al., 2013; Yakobi-Hancock et al., 2013; Wheeler et al., 2015). The size distribution of INPs did not drastically change between -25 and -30 °C (Fig. 6c and d), and the dominant mode in the surface area distribution of airborne mineral dust (Maring et al., 2003) can occur at approximately the same size range as biological INPs (Després et al., 2012). While in a very different ecosystem and climatic region, Prenni et al. (2009) noted that the relative contribution of mineral dust particles to the total number of INPs in the Amazon region increased as ice nucleation temperature decreased. Only below -27 °C did the amount of mineral dust significantly influence the number of INPs, while above this temperature most INPs were biological (Prenni et al., 2009). Ten-day back trajectories initiated at the midpoint of each INP sampling period are available in Fig. S2 of the Supplement. None of the trajectories pass over major arid regions in Asia or Africa; however, this does not rule out mineral dust or soils as a source of INPs in our measurements.

### 3.6 Do the potential sources of ice nuclei change with air mass classification?

In the preceding sections we did not differentiate data based on air mass classification. Here we present correlations within each of the four air mass categories introduced in Sect. 2.8 to investigate if the major sources of INPs vary with air mass type. The correlations for each air mass type are given in Table 2. Correlations involving sodium and MSA are not included due to insufficient data, and only statistically significant correlations will be discussed ($P < 0.05$).

The general trends presented in Table 1 for the undifferentiated data are also found in Table 2 for the various air mass categories. In coastal NW, Pacific Ocean, and free tropospheric air masses, INP number concentrations are well correlated to those of fluorescent bioparticles at temperatures between -15 and -25 °C with $R$ values ranging from 0.64 to 0.99 (an average of 0.89), and in free tropospheric air masses a very strong correlation is also found at -30 °C ($R$ =

500 1.00). In most cases, these are the strongest correlations noted at a given temperature. This again
501 suggests that many INPs may have been biological.

502 In coastal NW and free tropospheric air masses, INPs and total particles are also closely
503 correlated. These correlations are strong in the case of coastal NW air masses at ice activation
504 temperatures of -15 to -25 °C ($R$ = 0.70–0.85) and very strong in air masses from the free
505 troposphere between -20 and -30 °C ($R$ = 0.98–0.99). The correlation coefficients are
506 significantly greater than those found in the undifferentiated data of Table 1. With the average
507 fraction of particles that exhibited fluorescence in these air masses being close to the campaign
508 average, the good correlations with total particles suggest that non-biological INPs such as
509 mineral dust may have also contributed to the INP population.

510 Correlations of INPs with eBC are strong ($R$ = 0.71–0.84) at -25 °C and above in coastal
511 NW air masses and very strong ($R$ = 0.99) at -15 °C in air masses from the free troposphere.
512 Correlations of INPs with CO and $SO_2$ in these air masses are also moderate to very strong in
513 some cases (see Table S3 of the Supplement). However, more than 84 and 100 % of INPs active
514 at these temperatures were larger than 1 μm in size in air masses from the coastal NW and the
515 free troposphere, respectively. Vegetation NW of the sampling site closely follows that of the
516 region, and potential sources of supermicron INPs from the coastal NW include forests of coastal
517 western hemlock. Given the dominance of supermicron INPs in these two air mass types, it is
518 unlikely that BC was an important source of INPs.

519 **3.7 Can existing parameterizations accurately predict measured INP concentrations?**

520 Empirical parameterizations have been developed to predict ice nucleation in atmospheric
521 models. Here we investigate whether or not a number of these parameterizations are consistent
522 with the current measurements. In total we tested six different parameterizations: those of

523 Fletcher (1962), hereafter F62; Cooper (1986), hereafter C86; Meyers et al. (1992), hereafter
524 M92; DeMott et al. (2010), hereafter D10; and two from Tobo et al. (2013), hereafter $T13_{total}$ and
525 $T13_{fluorescent}$. Details on these parameterizations are given in the Supplement.

526 In Fig. 8 we compare measured INP number concentrations with predicted INP number
527 concentrations based on the parameterizations discussed above. The parameterizations of D10,
528 $T13_{total}$ and $T13_{fluorescent}$ require knowledge of either total particle or fluorescent bioparticle
529 number concentrations with sizes > 0.5 μm. Here we use the data from the WIBS-4A over its full
530 size range (0.5–23.7 μm) to better match the sampling conditions used in D10 and T13. Note that
531 the parameterization of $T13_{fluorescent}$ based on fluorescent bioparticle number concentrations was
532 formulated using measurements from an ultraviolet aerodynamic particle sizer (UV-APS),
533 whereas this study uses a WIBS-4A. As noted in Healy et al. (2014), there may be discrepancies
534 between the number concentrations of fluorescent bioparticles detected by the UV-APS and
535 WIBS-4A. With more fluorescent channels and more sensitive electronics, the WIBS-4A may
536 probe different fluorophores than the UV-APS, thus detecting greater concentrations of
537 fluorescent bioparticles and in turn leading to greater predicted INP number concentrations.
538 Also, the INP number concentrations measured by the MOUDI-DFT are for particle sizes of
539 0.18–10 μm, whereas the INP measurements used to formulate the parameterizations of M92,
540 D10, and T13 were for particles ≤ 3, ≤ 1.6, and ≤ 2.4 μm, respectively. As a result, when
541 reporting measured INP number concentrations in Fig. 8 we limit the MOUDI-DFT data to
542 particle sizes that overlap with those used to formulate the parameterizations (see the
543 Supplement for details).

544 It is evident in Fig. 8 that none of the parameterizations are able to consistently predict
545 the measured INP number concentrations within a factor or 5 over the entire temperature range

546 investigated. The most accurate parameterization is that of C86 (Fig. 8b), predicting 25 % and 57
547 % of the INP number concentrations within a factor of 2 and 5, respectively, of the solid 1:1 line.
548 While the C86 parameterization works reasonably well at temperatures of -15 to -25 °C, at lower
549 temperatures it becomes increasingly inaccurate, possibly due to it being applied outside the
550 temperature range over which it was developed (-5 to -25 °C).

551 The parameterizations of D10, $T13_{total}$ and $T13_{fluorescent}$ incorporate measurements of total
552 particles or fluorescent bioparticles, but are found to be poor predictors of the values measured in
553 this study as on average only 41% of INP number concentrations are predicted within a factor of
554 5 (Fig. 8d–f). A number of datasets from diverse locations were used in the development of the
555 D10 parameterization, but those with a strong marine influence were not included because sea
556 salt is not known to be an efficient ice nucleus under the conditions investigated (immersion
557 freezing at temperatures above -35 °C). Given the proximity of our sampling site to the Pacific
558 Ocean (Fig. 1) and the back trajectories of the sampled air masses (Fig. 2), a marine influence in
559 our samples may contribute to the somewhat poor performance of the D10 parameterization and
560 the over-estimation of INPs shown in Fig. 8d. The $T13_{total}$ and $T13_{fluorescent}$ parameterizations
561 were developed using data from a forested site in Colorado. Differences in the composition,
562 concentration, and ice-nucleating ability of both biological and non-biological particles between
563 the continental forest of T13 and the coastal site of this study may have contributed to the
564 inaccuracy of the $T13_{total}$ and $T13_{fluorescent}$ parameterizations (Fig. 8e–f).

565 Figure 8 suggests that additional measurements of INPS in other environments, times of
566 year, and altitudes are needed to further test and improve current empirical parameterizations of
567 INPs. The results presented in Fig. 8 also indicate that the application of INP parameterizations

568 to locations dissimilar to that of the original study used to generate the parameterizations should
569 be done with care.

570 **4. Summary and conclusions**

571 The number concentrations of 0.18–10 μm INPs active in the immersion mode were
572 determined at a coastal site in Western Canada during the summer of 2013 as part of the
573 NETCARE project. We investigated the strength of linear correlations between these INP values
574 and measurements of total particles, fluorescent bioparticles, eBC, sodium, MSA, and wind
575 speed and also compared their size distributions where these measurements were available. We
576 found that (1) biological particles, possibly from local vegetation, were likely the major source of
577 ice nuclei at freezing temperatures between -15 and -25 °C; (2) non-biological particles such as
578 mineral dust may also have had an important contribution to the population of INPs active at -30
579 °C; (3) the prevalence of supermicron INPs makes BC particles an unlikely source of ice nuclei;
580 and (4) there was no evidence of marine particles being a significant source of ice nuclei,
581 although the ocean as a source of INPs cannot be ruled out. One possibility is that biological
582 INPs released by nearby vegetation were present in sufficient numbers at this site to overwhelm
583 the presence of any INPs from the ocean.

584 Six empirical parameterizations of ice nucleation for use in atmospheric models were
585 tested to determine the accuracy with which they predict INP number concentrations at this
586 coastal site. Overall, none of the parameterizations were found to be suitable, predicting only 1 to
587 57 % of INPs within a factor of 5 of the measured value. This highlights the need for the
588 development of INP parameterizations that are appropriate for this complex environment.

589 In this paper we assumed that particles were externally mixed. In future studies it would
590 be useful to include mixing state measurements together with studies similar to those presented

here to quantify the extent of external versus internal mixing. In addition, studies that identify INPs followed by chemical composition measurements of these particles by electron microscopy (e.g. Knopf et al., 2014) or fluorescence microscopy would be useful to supplement the information gained from correlation analyses of collocated instruments.

**Acknowledgements**

The authors thank K. Bach, O. Greiner, J. Hansen, A. Klady, K. Love, D. Lovrity, T. Mittertreiner, R. Neagu, P. Padhiar for designing and constructing the NETCARE mobile laboratory used in this study, A. Chivulescu for assistance with ion chromatography measurements, D. O'Connor for assistance analyzing and interpreting WIBS-4A measurements, and L. A. Miller for helpful discussions. The sampling site at Amphitrite Point is located at a Coast Guard station and we would like to thank the Department of Fisheries and Oceans and all the staff at the site for their help. The site is jointly supported and maintained by Environment Canada, the British Columbia Ministry of Environment, and Metro Vancouver. The Natural Sciences and Engineering Research Council of Canada supported this research through its Climate Change and Atmospheric Research program. The authors gratefully acknowledge the NOAA Air Resources Laboratory (ARL) for the provision of the HYSPLIT transport and dispersion model and READY website (http://www.ready.noaa.gov) used in this publication. J. A. Huffman and J. Li acknowledge internal faculty support from the Division of Natural Sciences and Math and PROF grant support from the Office of Research and Sponsored Programs at the University of Denver.

## References


Alpert, P. A., Aller, J. Y. and Knopf, D. A.: Ice nucleation from aqueous NaCl droplets with and without marine diatoms, Atmos. Chem. Phys., 11, 5539–5555, doi:10.5194/acp-11-5539-2011, 2011.

Andreae, M. O., Ferek, R. J., Bermond, F., Byrd, K. P., Engstrom, R. T., Hardin, S., Houmere, P. D., LeMarrec, F., Raemdonck, H. and Chatfield, R. B.: Dimethyl sulfide in the marine atmosphere, J. Geophys. Res., 90, 12891–12900, doi:10.1029/JD090iD07p12891, 1985.

Andreas, E. L.: A New Sea Spray Generation Function for Wind Speeds up to 32 m $s^{-1}$, J. Phys. Oceanogr., 28, 2175–2184, 1998.

Atkinson, J. D., Murray, B. J., Woodhouse, M. T., Whale, T. F., Baustian, K. J., Carslaw, K. S., Dobbie, S., O'Sullivan, D. and Malkin, T. L.: The importance of feldspar for ice nucleation by mineral dust in mixed-phase clouds, Nature, 498, 355–358, doi:10.1038/nature12278, 2013.

Augustin, S., Wex, H., Niedermeier, D., Pummer, B., Grothe, H., Hartmann, S., Tomsche, L., Clauss, T., Voigtländer, J., Ignatius, K. and Stratmann, F.: Immersion freezing of birch pollen washing water, Atmos. Chem. Phys., 13, 10989–11003, doi:10.5194/acp-13-10989-2013, 2013.

Austin, M. A., Buffet, D. A., Nicholson, D. J. and Scudder, G. G. E.: Taking Natures Pulse: The Status of Biodiversity in British Columbia, Biodiversity BC, Victoria, available at: http://www.biodiversitybc.org (last access: 10 October 2014), 2008.

Baker, M. B.: Cloud Microphysics and Climate, Science, 276, 1072–1078, doi:10.1126/science.276.5315.1072, 1997.

Bates, T. S., Calhoun, J. A. and Quinn, P. K.: Variations in the methanesulfonate to sulfate molar ratio in submicrometer marine aerosol particles over the South Pacific Ocean, J. Geophys. Res. Ocean., 97, 9859–9865, doi:10.1029/92JD00411, 1992.

Becagli, S., Lazzara, L., Fani, F., Marchese, C., Traversi, R., Severi, M., di Sarra, A., Sferlazzo, D., Piacentino, S., Bommarito, C., Dayan, U. and Udisti, R.: Relationship between methanesulfonate ($MS^-$) in atmospheric particulate and remotely sensed phytoplankton activity in oligo-mesotrophic central Mediterranean Sea, Atmos. Environ., 79, 681–688, doi:10.1016/j.atmosenv.2013.07.032, 2013.

Blanchard, D. C.: The electrification of the atmosphere by particles from bubbles in the sea, Prog. Oceanogr., 1, 73–202, doi:10.1016/0079-6611(63)90004-1, 1963.

Blanchard, D. C.: The ejection of drops from the sea and their enrichment with bacteria and other materials: A review, Estuaries, 12, 127–137, doi:10.2307/1351816, 1989.

Blanchard, D. C. and Woodcock, A. H.: Bubble formation and modification in the sea and its meteorological significance, Tellus, 9, 145–158, doi:10.1111/j.2153-3490.1957.tb01867.x, 1957.

Bones, D. L., Henricksen, D. K., Mang, S. A., Gonsior, M., Bateman, A. P., Nguyen, T. B., Cooper, W. J. and Nizkorodov, S. A.: Appearance of strong absorbers and fluorophores in limonene-$O_3$ secondary organic aerosol due to $NH_4^+$-mediated chemical aging over long time scales, J. Geophys. Res., 115, D05203, doi:10.1029/2009JD012864, 2010.

651 Boucher, O., Randall, D., Artaxo, P., Bretherton, C., Feingold, G., Foster, P., Kerminen, V.-M.,
652 Kondo, Y., Liao, H., Lohmann, U., Rasch, P., Satheesh, S. K., Sherwood, S., Stevens, B. and
653 Zhang, X. Y.: Clouds and Aerosols, in Climate Change 2013: The Physical Science Basis.
654 Contribution of Working Group I to the Fifth Assessment Report of the Intergovernmental Panel
655 on Climate Change, edited by T. F. Stocker, D. Qin, G.-K. Plattner, M. Tignor, S. K. Allen, J.
656 Boschung, A. Nauels, Y. Xia, V. Bex, and P. M. Midgley, Cambridge University Press,
657 Cambridge, United Kingdom and New York, NY, USA, 2013.

658 Broadley, S. L., Murray, B. J., Herbert, R. J., Atkinson, J. D., Dobbie, S., Malkin, T. L.,
659 Condliffe, E. and Neve, L.: Immersion mode heterogeneous ice nucleation by an illite rich
660 powder representative of atmospheric mineral dust, Atmos. Chem. Phys., 12, 287–307,
661 doi:10.5194/acp-12-287-2012, 2012.

662 Brooks, S. D., Suter, K. and Olivarez, L.: Effects of Chemical Aging on the Ice Nucleation
663 Activity of Soot and Polycyclic Aromatic Hydrocarbon Aerosols, J. Phys. Chem. A, 118, 10036–
664 10047, doi:10.1021/jp508809y, 2014.

665 Burrows, S. M., Hoose, C., Pöschl, U. and Lawrence, M. G.: Ice nuclei in marine air: biogenic
666 particles or dust?, Atmos. Chem. Phys., 13, 245–267, doi:10.5194/acp-13-245-2013, 2013.

667 Carlile, M. J., Watkinson, S. C. and Gooday, G. W.: The Fungi, Second Edi., Academic Press,
668 London, United Kingdom and San Diego, CA, USA, 2001.

669 Charlson, R. J., Lovelock, J. E., Andreae, M. O. and Warren, S. G.: Oceanic phytoplankton,
670 atmospheric sulphur, cloud albedo and climate, Nature, 326, 655–661, doi:10.1038/326655a0,
671 1987.

672 Chou, C., Stetzer, O., Weingartner, E., Jurányi, Z., Kanji, Z. A. and Lohmann, U.: Ice nuclei
673 properties within a Saharan dust event at the Jungfraujoch in the Swiss Alps, Atmos. Chem.
674 Phys., 11, 4725–4738, doi:10.5194/acp-11-4725-2011, 2011.

675 Christner, B. C., Morris, C. E., Foreman, C. M., Cai, R. and Sands, D. C.: Ubiquity of Biological
676 Ice Nucleators in Snowfall, Science, 319, 1214, doi:10.1126/science.1149757, 2008.

677 Conen, F., Morris, C. E., Leifeld, J., Yakutin, M. V and Alewell, C.: Biological residues define
678 the ice nucleation properties of soil dust, Atmos. Chem. Phys., 11, 9643–9648, doi:10.5194/acp-
679 11-9643-2011, 2011.

680 Cooper, W. A.: Ice initiation in natural clouds, Meteor. Mon., 21, 29–32, doi:10.1175/0065-
681 9401-21.43.29, 1986.

682 Corbin, J. C., Rehbein, P. J. G., Evans, G. J. and Abbatt, J. P. D.: Combustion particles as ice
683 nuclei in an urban environment: Evidence from single-particle mass spectrometry, Atmos.
684 Environ., 51, 286–292, doi:10.1016/j.atmosenv.2012.01.007, 2012.

685 Costa, T. S., Gonçalves, F. L. T., Yamasoe, M. A., Martins, J. A. and Morris, C. E.: Bacterial ice
686 nuclei impact cloud lifetime and radiative properties and reduce atmospheric heat loss in the
687 BRAMS simulation model, Environ. Res. Lett., 9, 084020, doi:10.1088/1748-9326/9/8/084020,
688 2014.

689 Cozic, J., Mertes, S., Verheggen, B., Cziczo, D. J., Gallavardin, S. J., Walter, S., Baltensperger,
690 U. and Weingartner, E.: Black carbon enrichment in atmospheric ice particle residuals observed

691 in lower tropospheric mixed phase clouds, J. Geophys. Res., 113, D15209,
692 doi:10.1029/2007JD009266, 2008.

693 Creamean, J. M., Suski, K. J., Rosenfeld, D., Cazorla, A., DeMott, P. J., Sullivan, R. C., White,
694 A. B., Ralph, F. M., Minnis, P., Comstock, J. M., Tomlinson, J. M. and Prather, K. A.: Dust and
695 Biological Aerosols from the Sahara and Asia Influence Precipitation in the Western U.S.,
696 Science, 339, 1572–1578, doi:10.1126/science.1227279, 2013.

697 Cziczo, D. J., Froyd, K. D., Hoose, C., Jensen, E. J., Diao, M., Zondlo, M. A., Smith, J. B.,
698 Twohy, C. H. and Murphy, D. M.: Clarifying the Dominant Sources and Mechanisms of Cirrus
699 Cloud Formation, Science, 340, 1320–1324, doi:10.1126/science.1234145, 2013.

700 Cziczo, D. J., Murphy, D. M., Hudson, P. K. and Thomson, D. S.: Single particle measurements
701 of the chemical composition of cirrus ice residue during CRYSTAL-FACE, J. Geophys. Res.,
702 109, D04201, doi:10.1029/2003JD004032, 2004.

703 Dancey, C. P. and Reidy, J.: Statistics Without Maths for Psychology, Pearson Education
704 Limited, Essex, England, 2011.

705 DeMott, P. J., Hill, T. C. J., McCluskey, C. S., Prather, K. A., Collins, D. B., Sullivan, R. C.,
706 Ruppel, M. J., Mason, R. H., Irish, V. E., Lee, T., Hwang, C. Y., Rhee, T. S., Snider, J. R.,
707 McMeeking, G. R., Dhaniyala, S., Lewis, E. R., Wentzell, J., Abbatt, J. P. D., Lee, C., Sultana,
708 C. M., Ault, A. P., Axson, J. I., Martinez, M. D., Venero, I., Figueroa, G. S., Stokes, M. D.,
709 Deane, G. B., Mayol-Bracero, O. L., Grassian, V. H., Bertram, T. H., Bertram, A. K., Moffett, B.
710 F. and Franc, G. D.: Sea spray aerosol as a unique source of ice nucleating particles, submitted,
711 2015.

712 DeMott, P. J., Petters, M. D., Prenni, A. J., Carrico, C. M., Kreidenweis, S. M., Collett Jr., J. L.
713 and Moosmüller, H.: Ice nucleation behavior of biomass combustion particles at cirrus
714 temperatures, J. Geophys. Res., 114, D16205, doi:10.1029/2009JD012036, 2009.

715 DeMott, P. J., Prenni, A. J., Liu, X., Kreidenweis, S. M., Petters, M. D., Twohy, C. H.,
716 Richardson, M. S., Eidhammer, T. and Rogers, D. C.: Predicting global atmospheric ice nuclei
717 distributions and their impacts on climate, P. Natl. Acad. Sci. USA, 107, 11217–11222,
718 doi:10.1073/pnas.0910818107, 2010.

719 DeMott, P. J., Sassen, K., Poellot, M. R., Baumgardner, D., Rogers, D. C., Brooks, S. D., Prenni,
720 A. J. and Kreidenweis, S. M.: African dust aerosols as atmospheric ice nuclei, Geophys. Res.
721 Lett., 30, 1732, doi:10.1029/2003GL017410, 2003.

722 Després, V. R., Huffman, J. A., Burrows, S. M., Hoose, C., Safatov, A. S., Buryak, G., Fröhlich-
723 Nowoisky, J., Elbert, W., Andreae, M. O., Pöschl, U. and Jaenicke, R.: Primary biological
724 aerosol particles in the atmosphere: a review, Tellus B, 64, 15598,
725 doi:10.3402/tellusb.v64i0.15598, 2012.

726 Diehl, K., Matthias-Maser, S., Jaenicke, R. and Mitra, S. K.: The ice nucleating ability of pollen:
727 Part II. Laboratory studies in immersion and contact freezing modes, Atmos. Res., 61, 125–133,
728 doi:10.1016/S0169-8095(01)00132-6, 2002.

729 Diehl, K., Quick, C., Matthias-Maser, S., Mitra, S. K. and Jaenicke, R.: The ice nucleating ability
730 of pollen: Part I. Laboratory studies in deposition and condensation freezing modes, Atmos. Res.,
731 58, 75–87, doi:10.1016/S0169-8095(01)00091-6, 2001.

Draxler, R. R. and Rolph, G. D.: HYSPLIT (HYbrid Single-Particle Lagrangian Integrated Trajectory) Model access via NOAA ARL READY Website, available at: http://ready.arl.noaa.gov/HYSPLIT.php (last access: 27 May 2014), NOAA Air Resources Laboratory, Silver Spring, MD, 2014.

Dymarska, M., Murray, B. J., Sun, L., Eastwood, M. L., Knopf, D. A. and Bertram, A. K.: Deposition ice nucleation on soot at temperatures relevant for the lower troposphere, J. Geophys. Res., 111, D04204, doi:10.1029/2005JD006627, 2006.

Ebert, M., Worringen, A., Benker, N., Mertes, S., Weingartner, E. and Weinbruch, S.: Chemical composition and mixing-state of ice residuals sampled within mixed phase clouds, Atmos. Chem. Phys., 11, 2805–2816, doi: 10.5194/acp-11-2805-2011, 2011.

Field, P. R., Heymsfield, A. J., Shipway, B. J., DeMott, P. J., Pratt, K. A., Rogers, D. C., Stith, J. and Prather, K. A.: Ice in Clouds Experiment-Layer Clouds. Part II: Testing Characteristics of Heterogeneous Ice Formation in Lee Wave Clouds, J. Atmos. Sci., 69, 1066–1079, doi:10.1175/JAS-D-11-026.1, 2012.

Field, P. R., Möhler, O., Connolly, P., Krämer, M., Cotton, R., Heymsfield, A. J., Saathoff, H. and Schnaiter, M.: Some ice nucleation characteristics of Asian and Saharan desert dust, Atmos. Chem. Phys., 6, 2991–3006, doi:10.5194/acp-6-2991-2006, 2006.

Fletcher, N. H.: The Physics of Rainclouds, Cambridge University Press, Cambridge, United Kingdom, 1962.

Friedman, B., Kulkarni, G., Beránek, J., Zelenyuk, A., Thornton, J. A. and Cziczo, D. J.: Ice nucleation and droplet formation by bare and coated soot particles, J. Geophys. Res., 116, D17203, doi:10.1029/2011JD015999, 2011.

Fröhlich-Nowoisky, J., Hill, T. C. J., Pummer, B. G., Yordanova, P., Franc, G. D. and Pöschl, U.: Ice nucleation activity in the widespread soil fungus *Mortierella alpina*, Biogeosciences, 12, 1057–1071, doi:10.5194/bg-12-1057-2015, 2015.

Gabey, A. M., Gallagher, M. W., Whitehead, J., Dorsey, J. R., Kaye, P. H. and Stanley, W. R.: Measurements and comparison of primary biological aerosol above and below a tropical forest canopy using a dual channel fluorescence spectrometer, Atmos. Chem. Phys., 10, 4453–4466, doi:10.5194/acp-10-4453-2010, 2010.

Gabey, A. M., Stanley, W. R., Gallagher, M. W. and Kaye, P. H.: The fluorescence properties of aerosol larger than 0.8 μm in urban and tropical rainforest locations, Atmos. Chem. Phys., 11, 5491–5504, doi:10.5194/acp-11-5491-2011, 2011.

Gadi, R., Kulshrestha, U. C., Sarkar, A. K., Garg, S. C. and Parashar, D. C.: Emissions of $SO_2$ and $NO_x$ from biofuels in India, Tellus B, 55, 787–795, doi:10.1034/j.1600-0889.2003.00065.x, 2003.

Galanter, M., Levy II, H. and Carmichael, G. R.: Impacts of biomass burning on tropospheric CO, $NO_x$, and $O_3$, J. Geophys. Res., 105, 6633–6653, doi:10.1029/1999JD901113, 2000.

Garcia, E., Hill, T. C. J., Prenni, A. J., DeMott, P. J., Franc, G. D. and Kreidenweis, S. M.: Biogenic ice nuclei in boundary layer air over two U.S. High Plains agricultural regions, J. Geophys. Res., 117, D18209, doi:10.1029/2012JD018343, 2012.

772 Gaston, C. J., Pratt, K. A., Qin, X. and Prather, K. A.: Real-Time Detection and Mixing State of
773 Methanesulfonate in Single Particles at an Inland Urban Location during a Phytoplankton
774 Bloom, Environ. Sci. Technol., 44, 1566–1572, doi:10.1021/es902069d, 2010.

775 Gorbunov, B., Baklanov, A., Kakutkina, N., Windsor, H. L. and Toumi, R.: Ice nucleation on
776 soot particles, J. Aerosol Sci., 32, 199–215, doi:10.1016/s0021-8502(00)00077-x, 2001.

777 Hader, J. D., Wright, T. P. and Petters, M. D.: Contribution of pollen to atmospheric ice nuclei
778 concentrations, Atmos. Chem. Phys., 14, 5433–5449, doi:10.5194/acp-14-5433-2014, 2014.

779 Haga, D. I., Burrows, S. M., Iannone, R., Wheeler, M. J., Mason, R. H., Chen, J., Polishchuk, E.
780 A., Pöschl, U. and Bertram, A. K.: Ice nucleation by fungal spores from the classes
781 *Agaricomycetes*, *Ustilaginomycetes*, and *Eurotiomycetes*, and the effect on the atmospheric
782 transport of these spores, Atmos. Chem. Phys., 14, 8611–8630, doi:10.5194/acp-14-8611-2014,
783 2014.

784 Haga, D. I., Iannone, R., Wheeler, M. J., Mason, R., Polishchuk, E. A., Fetch Jr., T., van der
785 Kamp, B. J., McKendry, I. G. and Bertram, A. K.: Ice nucleation properties of rust and bunt
786 fungal spores and their transport to high altitudes, where they can cause heterogeneous freezing,
787 J. Geophys. Res.-Atmos., 118, 7260–7272, doi:10.1002/jgrd.50556, 2013.

788 Healy, D. A., Huffman, J. A., O'Connor, D. J., Pöhlker, C., Pöschl, U. and Sodeau, J. R.:
789 Ambient measurements of biological aerosol particles near Killarney, Ireland: a comparison
790 between real-time fluorescence and microscopy techniques, Atmos. Chem. Phys., 14, 8055–
791 8069, doi:10.5194/acp-14-8055-2014, 2014.

792 Healy, D. A., O'Connor, D. J., Burke, A. M. and Sodeau, J. R.: A laboratory assessment of the
793 Waveband Integrated Bioaerosol Sensor (WIBS-4) using individual samples of pollen and fungal
794 spore material, Atmos. Environ., 60, 534–543, doi:10.1016/j.atmosenv.2012.06.052, 2012a.

795 Healy, D. A., O'Connor, D. J. and Sodeau, J. R.: Measurement of the particle counting efficiency
796 of the "Waveband Integrated Bioaerosol Sensor" model number 4 (WIBS-4), J. Aerosol Sci., 47,
797 94–99, doi:10.1016/j.jaerosci.2012.01.003, 2012b.

798 Hill, T. C. J., Moffett, B. F., DeMott, P. J., Georgakopoulos, D. G., Stump, W. L. and Franc, G.
799 D.: Measurement of Ice Nucleation-Active Bacteria on Plants and in Precipitation by
800 Quantitative PCR, Appl. Environ. Microbiol., 80, 1256–1267, doi: 10.1128/AEM.02967-13,
801 2014.

802 Hiranuma, N., Möhler, O., Yamashita, K., Tajiri, T., Saito, A., Kiselev, A., Hoffmann, N.,
803 Hoose, C., Jantsch, E., Koop, T. and Murakami, M.: Ice nucleation by cellulose and its potential
804 contribution to ice formation in clouds, Nat. Geosci., 8, 273–277, doi:10.1038/ngeo2374, 2015.

805 Hoose, C., Kristjánsson, J. E. and Burrows, S. M.: How important is biological ice nucleation in
806 clouds on a global scale?, Environ. Res. Lett., 5, 024009, doi:10.1088/1748-9326/5/2/024009,
807 2010a.

808 Hoose, C., Kristjánsson, J. E., Chen, J.-P. and Hazra, A.: A Classical-Theory-Based
809 Parameterization of Heterogeneous Ice Nucleation by Mineral Dust, Soot, and Biological
810 Particles in a Global Climate Model, J. Atmos. Sci., 67, 2483–2503,
811 doi:10.1175/2010JAS3425.1, 2010b.

812 Hoose, C. and Möhler, O.: Heterogeneous ice nucleation on atmospheric aerosols: a review of
813 results from laboratory experiments, Atmos. Chem. Phys., 12, 9817–9854, doi:10.5194/acp-12-
814 9817-2012, 2012.

815 Huffman, J. A., Prenni, A. J., DeMott, P. J., Pöhlker, C., Mason, R. H., Robinson, N. H.,
816 Fröhlich-Nowoisky, J., Tobo, Y., Després, V. R., Garcia, E., Gochis, D. J., Harris, E., Müller-
817 Germann, I., Ruzene, C., Schmer, B., Sinha, B., Day, D. A., Andreae, M. O., Jimenez, J. L.,
818 Gallagher, M., Kreidenweis, S. M., Bertram, A. K. and Pöschl, U.: High concentrations of
819 biological aerosol particles and ice nuclei during and after rain, Atmos. Chem. Phys., 13, 6151–
820 6164, doi:10.5194/acp-13-6151-2013, 2013.

821 Huffman, J. A., Sinha, B., Garland, R. M., Snee-Pollmann, A., Gunthe, S. S., Artaxo, P., Martin,
822 S. T., Andreae, M. O. and Pöschl, U.: Size distributions and temporal variations of biological
823 aerosol particles in the Amazon rainforest characterized by microscopy and real-time UV-APS
824 fluorescence techniques during AMAZE-08, Atmos. Chem. Phys., 12, 11997–12019,
825 doi:10.5194/acp-12-11997-2012, 2012.

826 Huffman, J. A., Treutlein, B. and Pöschl, U.: Fluorescent biological aerosol particle
827 concentrations and size distributions measured with an Ultraviolet Aerodynamic Particle Sizer
828 (UV-APS) in Central Europe, Atmos. Chem. Phys., 10, 3215–3233, doi:10.5194/acp-10-3215-
829 2010, 2010.

830 Iannone, R., Chernoff, D. I., Pringle, A., Martin, S. T. and Bertram, A. K.: The ice nucleation
831 ability of one of the most abundant types of fungal spores found in the atmosphere, Atmos.
832 Chem. Phys., 11, 1191–1201, doi:10.5194/acp-11-1191-2011, 2011.

833 Jayaweera, K. and Flanagan, P.: Investigations on biogenic ice nuclei in the Arctic atmosphere,
834 Geophys. Res. Lett., 9, 94–97, doi:10.1029/GL009i001p00094, 1982.

835 Jiang, H., Yin, Y., Su, H., Shan, Y. and Gao, R.: The characteristics of atmospheric ice nuclei
836 measured at the top of Huangshan (the Yellow Mountains) in Southeast China using a newly
837 built static vacuum water vapor diffusion chamber, Atmos. Res., 153, 200–208,
838 doi:10.1016/j.atmosres.2014.08.015, 2015.

839 Joly, M., Amato, P., Deguillaume, L., Monier, M., Hoose, C. and Delort, A.-M.: Quantification
840 of ice nuclei active at near 0 °C temperatures in low-altitude clouds at the Puy de Dôme
841 atmospheric station, Atmos. Chem. Phys., 14, 8185–8195, doi:10.5194/acp-14-8185-2014, 2014.

842 Kamphus, M., Ettner-Mahl, M., Klimach, T., Drewnick, F., Keller, L., Cziczo, D. J., Mertes, S.,
843 Borrmann, S. and Curtius, J.: Chemical composition of ambient aerosol, ice residues and cloud
844 droplet residues in mixed-phase clouds: single particle analysis during the Cloud and Aerosol
845 Characterization Experiment (CLACE 6), Atmos. Chem. Phys., 10, 8077–8095,
846 doi:10.5194/acp-10-8077-2010, 2010.

847 Kanji, Z. A. and Abbatt, J. P. D.: Ice Nucleation onto Arizona Test Dust at Cirrus Temperatures:
848 Effect of Temperature and Aerosol Size on Onset Relative Humidity, J. Phys. Chem. A, 114,
849 935–941, doi:10.1021/jp908661m, 2010.

850 Kärcher, B., Möhler, O., DeMott, P. J., Pechtl, S. and Yu, F.: Insights into the role of soot
851 aerosols in cirrus cloud formation, Atmos. Chem. Phys., 7, 4203–4227, doi:10.5194/acp-7-4203-
852 2007, 2007.

853 Kaye, P., Stanley, W. R., Hirst, E., Foot, E. V, Baxter, K. L. and Barrington, S. J.: Single particle
854 multichannel bio-aerosol fluorescence sensor, Opt. Express, 13, 3583–3593,
855 doi:10.1364/OPEX.13.003583, 2005.

856 Keller, M. D.: Dimethyl Sulfide Production and Marine Phytoplankton: The Importance of
857 Species Composition and Cell Size, Biol. Oceanogr., 6, 375–382,
858 doi:10.1080/01965581.1988.10749540, 1989.

859 Kettle, A. J., Andreae, M. O., Amouroux, D., Andreae, T. W., Bates, T. S., Berresheim, H.,
860 Bingemer, H., Boniforti, R., Curran, M., DiTullio, G. R., Helas, G., Jones, G. B., Keller, M. D.,
861 Kiene, R. P., Leck, C., Levasseur, M., Malin, G., Maspero, M., Matrai, P., McTaggart, A. R.,
862 Mihalopoulos, N., Nguyen, B. C., Novo, A., Putaud, J. P., Rapsomanikis, S., Roberts, G.,
863 Schebeske, G., Sharma, S., Simó, R., Staubes, R., Turner, S. and Uher, G.: A global database of
864 sea surface dimethylsulfide (DMS) measurements and a procedure to predict sea surface DMS as
865 a function of latitude, longitude, and month, Glob. Biogeochem. Cy., 13, 399–444,
866 doi:10.1029/1999GB900004, 1999.

867 Klein, H., Nickovic, S., Haunold, W., Bundke, U., Nillius, B., Ebert, M., Weinbruch, S., Schuetz,
868 L., Levin, Z., Barrie, L. A. and Bingemer, H.: Saharan dust and ice nuclei over Central Europe,
869 Atmos. Chem. Phys., 10, 10211–10221, doi:10.5194/acp-10-10211-2010, 2010.

870 Knopf, D. A., Alpert, P. A., Wang, B. and Aller, J. Y.: Stimulation of ice nucleation by marine
871 diatoms, Nat. Geosci., 4, 88–90, doi:10.1038/ngeo1037, 2011.

872 Knopf, D. A., Alpert, P. A., Wang, B., O'Brien, R. E., Kelly, S. T., Laskin, A., Gilles, M. K. and
873 Moffet, R. C.: Microspectroscopic imaging and characterization of individually identified ice
874 nucleating particles from a case field study, J. Geophys. Res.-Atmos., 119, 10365–10381,
875 doi:10.1002/2014JD021866, 2014.

876 Knopf, D. A. and Koop, T.: Heterogeneous nucleation of ice on surrogates of mineral dust, J.
877 Geophys. Res., 111, D12201, doi:10.1029/2005JD006894, 2006.

878 Koop, T., Kapilashrami, A., Molina, L. T. and Molina, M. J.: Phase transitions of sea-salt/water
879 mixtures at low temperatures: Implications for ozone chemistry in the polar marine boundary
880 layer, J. Geophys. Res., 105, 26393–26402, doi:10.1029/2000JD900413, 2000.

881 Koop, T., Luo, B., Biermann, U. M., Crutzen, P. J. and Peter, T.: Freezing of $HNO_3/H_2SO_4/H_2O$
882 solutions at stratospheric temperatures: Nucleation statistics and experiments, J. Phys. Chem. A,
883 101, 1117–1133, doi:10.1021/jp9626531, 1997.

884 Kottek, M., Grieser, J., Beck, C., Rudolf, B. and Rubel, F.: World Map of the Köppen-Geiger
885 climate classification updated, Meteorol. Z., 15, 259–263, doi:10.1127/0941-2948/2006/0130,
886 2006.

887 Kozloff, L. M., Schofield, M. A. and Lute, M.: Ice nucleating activity of Pseudomonas syringae
888 and Erwinia herbicola, J. Bacteriol., 153, 222–231, 1983.

889 Kulkarni, G. and Dobbie, S.: Ice nucleation properties of mineral dust particles: determination of
890 onset $RH_i$, IN active fraction, nucleation time-lag, and the effect of active sites on contact angles,
891 Atmos. Chem. Phys., 10, 95–105, doi:10.5194/acp-10-95-2010, 2010.

892 Lee, H. J., Laskin, A., Laskin, J. and Nizkorodov, S. A.: Excitation-Emission Spectra and
893 Fluorescence Quantum Yields for Fresh and Aged Biogenic Secondary Organic Aerosols,
894 Environ. Sci. Technol., 47, 5763–5770, doi:10.1021/es400644c, 2013.

895 Leslie, J. F. and Summerell, B. A.: The *Fusarium* Laboratory Manual, Blackwell Publishing,
896 Ames, Iowa, USA, 2006.

897 Lin, J. C., Matsui, T., Pielke Sr., R. A. and Kummerow, C.: Effects of biomass-burning-derived
898 aerosols on precipitation and clouds in the Amazon Basin: a satellite-based empirical study, J.
899 Geophys. Res., 111, D19204, doi:10.1029/2005JD006884, 2006.

900 Lindow, S. E., Arny, D. C. and Upper, C. D.: Erwinia herbicola: A Bacterial Ice Nucleus Active
901 in Increasing Frost Injury to Corn, Phytopathology, 68, 523–527, 1978.

902 Liu, X., Penner, J. E. and Wang, M.: Influence of anthropogenic sulfate and black carbon on
903 upper tropospheric clouds in the NCAR CAM3 model coupled to the IMPACT global aerosol
904 model, J. Geophys. Res., 114, D03204, doi:10.1029/2008JD010492, 2009.

905 Lohmann, U.: A glaciation indirect aerosol effect caused by soot aerosols, Geophys. Res. Lett.,
906 29, 1052, doi:10.1029/2001GL014357, 2002.

907 Lüönd, F., Stetzer, O., Welti, A. and Lohmann, U.: Experimental study on the ice nucleation
908 ability of size-selected kaolinite particles in the immersion mode, J. Geophys. Res., 115,
909 D14201, doi:10.1029/2009JD012959, 2010.

910 Maheshwari, R.: Fungi: Experimental Methods in Biology, CRC Press, Taylor & Francis Group,
911 Boca Raton, Florida, USA, 2005.

912 Maki, L. R., Galyan, E. L., Chang-Chien, M.-M. and Caldwell, D. R.: Ice nucleation induced by
913 pseudomonas syringae, Appl. Microbiol., 28, 456–459, 1974.

914 Maki, L. R. and Willoughby, K. J.: Bacteria as Biogenic Sources of Freezing Nuclei, J. Appl.
915 Meteorol., 17, 1049–1053, 1978.

916 Marcolli, C., Gedamke, S., Peter, T. and Zobrist, B.: Efficiency of immersion mode ice
917 nucleation on surrogates of mineral dust, Atmos. Chem. Phys., 7, 5081–5091, doi:10.5194/acp-7-
918 5081-2007, 2007.

919 Maring, H., Savoie, D. L., Izaguirre, M. A., Custals, M. and Reid, J. S.: Mineral dust aerosol size
920 distribution change during atmospheric transport, J. Geophys. Res., 108, 8592,
921 doi:10.1029/2002JD002536, 2003.

922 Marple, V. A., Rubow, K. L. and Behm, S. M.: A Microorifice Uniform Deposit Impactor
923 (MOUDI): Description, Calibration, and Use, Aerosol Sci. Technol., 14, 434–446,
924 doi:10.1080/02786829108959504, 1991.

925 Mason, B. J. and Maybank, J.: Ice-nucleating properties of some natural mineral dusts, Q. J. R.
926 Meteorol. Soc., 84, 235–241, doi:10.1002/qj.49708436104, 1958.

927 Mason, R. H., Chou, C., McCluskey, C. S., Levin, E. J. T., Schiller, C. L., Hill, T. C. J.,
928 Huffman, J. A., DeMott, P. J. and Bertram, A. K.: The micro-orifice uniform deposit impactor-
929 droplet freezing technique (MOUDI-DFT) for measuring concentrations of ice nucleating
930 particles as a function of size: improvements and initial validation, Atmos. Meas. Tech., 8, 2449–
931 2462, doi:10.5194/amt-8-2449-2015, 2015.

McCluskey, C. S., DeMott, P. J., Prenni, A. J., Levin, E. J. T., McMeeking, G. R., Sullivan, A. P., Hill, T. C. J., Nakao, S., Carrico, C. M. and Kreidenweis, S. M.: Characteristics of atmospheric ice nucleating particles associated with biomass burning in the US: Prescribed burns and wildfires, J. Geophys. Res.-Atmos., 119, 10458–10470, doi:10.1002/2014JD021980, 2014.

McKendry, I. G., Christensen, E., Schiller, C. L., Vingarzan, R., Macdonald, A. M. and Li, Y.: Low Ozone Episodes at Amphitrite Point Marine Boundary Layer Observatory, British Columbia, Canada, Atmosphere-Ocean, 52, 271–280, doi:10.1080/07055900.2014.910164, 2014.

Meyers, M. P., DeMott, P. J. and Cotton, W. R.: New primary ice-nucleation parameterizations in an explicit cloud model, J. Appl. Meteorol., 31, 708–721, 1992.

Möhler, O., Büttner, S., Linke, C., Schnaiter, M., Saathoff, H., Stetzer, O., Wagner, R., Krämer, M., Mangold, A., Ebert, V. and Schurath, U.: Effect of sulfuric acid coating on heterogeneous ice nucleation by soot aerosol particles, J. Geophys. Res., 110, D11210, doi:10.1029/2004JD005169, 2005.

Möhler, O., DeMott, P. J., Vali, G. and Levin, Z.: Microbiology and atmospheric processes: the role of biological particles in cloud physics, Biogeosciences, 4, 1059–1071, doi:10.5194/bg-4-1059-2007, 2007.

Möhler, O., Field, P. R., Connolly, P., Benz, S., Saathoff, H., Schnaiter, M., Wagner, R., Cotton, R., Krämer, M., Mangold, A. and Heymsfield, A. J.: Efficiency of the deposition mode ice nucleation on mineral dust particles, Atmos. Chem. Phys., 6, 3007–3021, doi:10.5194/acp-6-3007-2006, 2006.

Monahan, E. C. and Muircheartaigh, I. Ó.: Optimal power-law description of oceanic whitecap coverage dependence on wind speed, J. Phys. Oceanogr., 10, 2094–2099, 1980.

Morris, C. E., Sands, D. C., Glaux, C., Samsatly, J., Asaad, S., Moukahel, A. R., Gonçalves, F. L. T. and Bigg, E. K.: Urediospores of rust fungi are ice nucleation active at > −10 °C and harbor ice nucleation active bacteria, Atmos. Chem. Phys., 13, 4223–4233, doi:10.5194/acp-13-4223-2013, 2013.

Morris, C. E., Sands, D. C., Vinatzer, B. A., Glaux, C., Guilbaud, C., Buffière, A., Yan, S., Dominguez, H. and Thompson, B. M.: The life history of the plant pathogen Pseudomonas syringae is linked to the water cycle, ISME J., 2, 321–334, doi: doi:10.1038/ismej.2007.113, 2008.

Murray, B. J., Broadley, S. L., Wilson, T. W., Atkinson, J. D. and Wills, R. H.: Heterogeneous freezing of water droplets containing kaolinite particles, Atmos. Chem. Phys., 11, 4191–4207, doi:10.5194/acp-11-4191-2011, 2011.

Murray, B. J., O'Sullivan, D., Atkinson, J. D. and Webb, M. E.: Ice nucleation by particles immersed in supercooled cloud droplets, Chem. Soc. Rev., 41, 6519–6554, doi:10.1039/c2cs35200a, 2012.

National Data Buoy Center, National Oceanic and Atmospheric Administration, http://www.ndbc.noaa.gov/station_page.php?station=46206 (last accessed: 9 December 2014), 2013.

Niedermeier, D., Hartmann, S., Shaw, R. A., Covert, D., Mentel, T. F., Schneider, J., Poulain, L., Reitz, P., Spindler, C., Clauss, T., Kiselev, A., Hallbauer, E., Wex, H., Mildenberger, K. and Stratmann, F.: Heterogeneous freezing of droplets with immersed mineral dust particles - measurements and parameterization, Atmos. Chem. Phys., 10, 3601–3614, doi:10.5194/acp-10-3601-2010, 2010.

O'Dowd, C. D. and de Leeuw, G.: Marine aerosol production: a review of the current knowledge, Philos. Trans. R. Soc. A, 365, 1753–1774, doi:10.1098/rsta.2007.2043, 2007.

O'Sullivan, D., Murray, B. J., Malkin, T. L., Whale, T. F., Umo, N. S., Atkinson, J. D., Price, H. C., Baustian, K. J., Browse, J. and Webb, M. E.: Ice nucleation by fertile soil dusts: relative importance of mineral and biogenic components, Atmos. Chem. Phys., 14, 1853–1867, doi:10.5194/acp-14-1853-2014, 2014.

O'Sullivan, D., Murray, B. J., Ross, J. F., Whale, T. F., Price, H. C., Atkinson, J. D., Umo, N. S. and Webb, M. E.: The relevance of nanoscale biological fragments for ice nucleation in clouds, Sci. Rep., 5, 8082, doi:10.1038/srep08082, 2015.

Pan, Y.-L., Holler, S., Chang, R. K., Hill, S. C., Pinnick, R. G., Niles, S., Bottiger, J. R. and Bronk, B. V: Real-time detection and characterization of individual flowing airborne biological particles: fluorescence spectra and elastic scattering measurements, P. Soc. Photo-Opt. Ins., 3855, 117–125, doi:10.1117/12.371270, 1999.

Parker, L. V, Sullivan, C. W., Forest, T. W. and Ackley, S. F.: Ice nucleation activity of antarctic marine microorganisms, Antarct. J. US, 20, 126–127, 1985.

Penner, J. E., Chen, Y., Wang, M. and Liu, X.: Possible influence of anthropogenic aerosols on cirrus clouds and anthropogenic forcing, Atmos. Chem. Phys., 9, 879–896, doi:10.5194/acp-9-879-2009, 2009.

Petzold, A., Kramer, H. and Schönlinner, M.: Continuous Measurement of Atmospheric Black Carbon Using a Multi-angle Absorption Photometer, Environ. Sci. Pollut. Res., 4, 78–82, 2002.

Petzold, A., Ogren, J. A., Fiebig, M., Laj, P., Li, S.-M., Baltensperger, U., Holzer-Popp, T., Kinne, S., Pappalardo, G., Sugimoto, N., Wehrli, C., Wiedensohler, A. and Zhang, X.-Y.: Recommendations for reporting "black carbon" measurements, Atmos. Chem. Phys., 13, 8365–8379, doi:10.5194/acp-13-8365-2013, 2013.

Petzold, A., Schloesser, H., Sheridan, P. J., Arnott, W. P., Ogren, J. A. and Virkkula, A.: Evaluation of Multiangle Absorption Photometry for Measuring Aerosol Light Absorption, Aerosol Sci. Technol., 39, 40–51, doi:10.1080/027868290901945, 2005.

Petzold, A. and Schönlinner, M.: Multi-angle absorption photometry - a new method for the measurement of aerosol light absorption and atmospheric black carbon, J. Aerosol Sci., 35, 421–441, doi:10.1016/j.jaerosci.2003.09.005, 2004.

Phillips, V. T. J., Andronache, C., Christner, B., Morris, C. E., Sands, D. C., Bansemer, A., Lauer, A., McNaughton, C. and Seman, C.: Potential impacts from biological aerosols on ensembles of continental clouds simulated numerically, Biogeosciences, 6, 987–1014, doi:10.5194/bg-6-987-2009, 2009.

Phinney, L., Leaitch, W. R., Lohmann, U., Boudries, H., Worsnop, D. R., Jayne, J. T., Toom-Sauntry, D., Wadleigh, M., Sharma, S. and Shantz, N.: Characterization of the aerosol over the

1013 sub-arctic north east Pacific Ocean, Deep-Sea Res. Pt. II, 53, 2410–2433,
1014 doi:10.1016/j.dsr2.2006.05.044, 2006.

1015 Pöhlker, C., Huffman, J. A. and Pöschl, U.: Autofluorescence of atmospheric bioaerosols -
1016 fluorescent biomolecules and potential interferences, Atmos. Meas. Tech., 5, 37–71,
1017 doi:10.5194/amt-5-37-2012, 2012.

1018 Pouleur, S., Richard, C., Martin, J.-G. and Antoun, H.: Ice Nucleation Activity in *Fusarium*
1019 *acuminatum* and *Fusarium avenaceum*, Appl. Environ. Microbiol., 58, 2960–2964, 1992.

1020 Prather, K. A., Bertram, T. H., Grassian, V. H., Deane, G. B., Stokes, M. D., DeMott, P. J.,
1021 Aluwihare, L. I., Palenik, B. P., Azam, F., Seinfeld, J. H., Moffet, R. C., Molina, M. J., Cappa,
1022 C. D., Geiger, F. M., Roberts, G. C., Russell, L. M., Ault, A. P., Baltrusaitis, J., Collins, D. B.,
1023 Corrigan, C. E., Cuadra-Rodriguez, L. A., Ebben, C. J., Forestieri, S. D., Guasco, T. L., Hersey,
1024 S. P., Kim, M. J., Lambert, W. F., Modini, R. L., Mui, W., Pedler, B. E., Ruppel, M. J., Ryder,
1025 O. S., Schoepp, N. G., Sullivan, R. C. and Zhao, D.: Bringing the ocean into the laboratory to
1026 probe the chemical complexity of sea spray aerosol, P. Natl. Acad. Sci. USA, 110, 7550–7555,
1027 doi:10.1073/pnas.1300262110, 2013.

1028 Pratt, K. A., DeMott, P. J., French, J. R., Wang, Z., Westphal, D. L., Heymsfield, A. J., Twohy,
1029 C. H., Prenni, A. J. and Prather, K. A.: In situ detection of biological particles in cloud ice-
1030 crystals, Nat. Geosci., 2, 398–401, doi:10.1038/ngeo521, 2009.

1031 Prenni, A. J., Petters, M. D., Kreidenweis, S. M., Heald, C. L., Martin, S. T., Artaxo, P., Garland,
1032 R. M., Wollny, A. G. and Pöschl, U.: Relative roles of biogenic emissions and Saharan dust as
1033 ice nuclei in the Amazon basin, Nat. Geosci., 2, 402–405, doi:10.1038/ngeo517, 2009.

1034 Prenni, A. J., Tobo, Y., Garcia, E., DeMott, P. J., Huffman, J. A., McCluskey, C. S.,
1035 Kreidenweis, S. M., Prenni, J. E., Pöhlker, C. and Pöschl, U.: The impact of rain on ice nuclei
1036 populations at a forested site in Colorado, Geophys. Res. Lett., 40, 227–231,
1037 doi:10.1029/2012GL053953, 2013.

1038 Pummer, B. G., Bauer, H., Bernardi, J., Bleicher, S. and Grothe, H.: Suspendable
1039 macromolecules are responsible for ice nucleation activity of birch and conifer pollen, Atmos.
1040 Chem. Phys., 12, 2541–2550, doi:10.5194/acp-12-2541-2012, 2012.

1041 Ribalet, F., Marchetti, A., Hubbard, K. A., Brown, K., Durkin, C. A., Morales, R., Robert, M.,
1042 Swalwell, J. E., Tortell, P. D. and Armbrust, E. V.: Unveiling a phytoplankton hotspot at a
1043 narrow boundary between coastal and offshore waters, P. Natl. Acad. Sci. USA, 107, 16571–
1044 16576, doi:10.1073/pnas.1005638107, 2010.

1045 Richard, C., Martin, J.-G. and Pouleur, S.: Ice nucleation activity identified in some
1046 phytopathogenic *Fusarium* species, Phytoprotection, 77, 83–92, doi:10.7202/706104ar, 1996.

1047 Richardson, M. S., DeMott, P. J., Kreidenweis, S. M., Cziczo, D. J., Dunlea, E. J., Jimenez, J. L.,
1048 Thomson, D. S., Ashbaugh, L. L., Borys, R. D., Westphal, D. L., Casuccio, G. S. and Lersch, T.
1049 L.: Measurements of heterogeneous ice nuclei in the western United States in springtime and
1050 their relation to aerosol characteristics, J. Geophys. Res., 112, D02209,
1051 doi:10.1029/2006JD007500, 2007.

1052 Rogers, D. C., DeMott, P. J., Kreidenweis, S. M. and Chen, Y.: Measurements of ice nucleating
1053 aerosols during SUCCESS, Geophys. Res. Lett., 25, 1383–1386, doi:10.1029/97GL03478, 1998.

Saltzman, E. S., Savoie, D. L., Prospero, J. M. and Zika, R. G.: Methanesulfonic acid and non-sea-salt sulfate in Pacific air: Regional and seasonal variations, J. Atmos. Chem., 4, 227–240, doi:10.1007/BF00052002, 1986.

Savoie, D. L., Prospero, J. M., Arimoto, R. and Duce, R. A.: Non-sea-salt sulfate and methanesulfonate at American Samoa, J. Geophys. Res., 99, 3587–3596, doi:10.1029/93JD03337, 1994.

Schnell, R. C.: Ice nuclei produced by laboratory cultured marine phytoplankton, Geophys. Res. Lett., 2, 500–502, doi:10.1029/GL002i011p00500, 1975.

Schnell, R. C.: Ice Nuclei in Seawater, Fog Water and Marine Air off the Coast of Nova Scotia: Summer 1975, J. Atmos. Sci., 34, 1299–1305, 1977.

Schnell, R. C. and Vali, G.: Freezing nuclei in marine waters, Tellus, 27, 321–323, doi:10.1111/j.2153-3490.1975.tb01682.x, 1975.

Schroder, J. C., Hanna, S. J., Modini, R. L., Corrigan, A. L., Kreidenweis, S. M., Macdonald, A. M., Noone, K. J., Russell, L. M., Leaitch, W. R. and Bertram, A. K.: Size-resolved observations of refractory black carbon particles in cloud droplets at a marine boundary layer site, Atmos. Chem. Phys., 15, 1367–1383, doi:10.5194/acp-15-1367-2015, 2015.

Schwarz, J. P., Gao, R. S., Perring, A. E., Spackman, J. R. and Fahey, D. W.: Black carbon aerosol size in snow, Sci. Rep., 3, 1356, doi:10.1038/srep01356, 2013.

Schwarz, J. P., Gao, R. S., Spackman, J. R., Watts, L. A., Thomson, D. S., Fahey, D. W., Ryerson, T. B., Peischl, J., Holloway, J. S., Trainer, M., Frost, G. J., Baynard, T., Lack, D. A., de Gouw, J. A., Warneke, C. and Del Negro, L. A.: Measurement of the mixing state, mass, and optical size of individual black carbon particles in urban and biomass burning emissions, Geophys. Res. Lett., 35, L13810, doi:10.1029/2008GL033968, 2008.

Sesartic, A., Lohmann, U. and Storelvmo, T.: Modelling the impact of fungal spore ice nuclei on clouds and precipitation, Environ. Res. Lett., 8, 014029, doi:10.1088/1748-9326/8/1/014029, 2013.

Sivaprakasam, V., Huston, A., Scotto, C. and Eversole, J.: Multiple UV wavelength excitation and fluorescence of bioaerosols, Opt. Express, 12, 4457–4466, doi:10.1364/OPEX.12.004457, 2004.

Sorooshian, A., Padró, L. T., Nenes, A., Feingold, G., McComiskey, A., Hersey, S. P., Gates, H., Jonsson, H. H., Miller, S. D., Stephens, G. L., Flagan, R. C. and Seinfeld, J. H.: On the link between ocean biota emissions, aerosol, and maritime clouds: Airborne, ground, and satellite measurements off the coast of California, Global Biogeochem. Cycles, 23, GB4007, doi:10.1029/2009GB003464, 2009.

Spracklen, D. V and Heald, C. L.: The contribution of fungal spores and bacteria to regional and global aerosol number and ice nucleation immersion freezing rates, Atmos. Chem. Phys., 14, 9051–9059, doi:10.5194/acp-14-9051-2014, 2014.

Statistics Canada, Catalogue no. 98-316-XWE, available at: http://www12.statcan.gc.ca/census-recensement/2011/dp-pd/prof/index.cfm?Lang=E (last access: 4 November 2014), Ottawa, 2012.

Storelvmo, T., Hoose, C. and Eriksson, P.: Global modeling of mixed-phase clouds: The albedo and lifetime effects of aerosols, J. Geophys. Res., 116, D05207, doi:10.1029/2010JD014724, 2011.

Sun, J., Ariya, P. A., Leighton, H. G. and Yau, M. K.: Modeling Study of Ice Formation in Warm-Based Precipitating Shallow Cumulus Clouds, J. Atmos. Sci., 69, 3315–3335, doi:10.1175/JAS-D-11-0344.1, 2012.

Szyrmer, W. and Zawadzki, I.: Biogenic and anthropogenic sources of ice-forming nuclei: A review, B. Am. Meteorol. Soc., 78, 209–228, 1997.

Tobo, Y., DeMott, P. J., Hill, T. C. J., Prenni, A. J., Swoboda-Colberg, N. G., Franc, G. D. and Kreidenweis, S. M.: Organic matter matters for ice nuclei of agricultural soil origin, Atmos. Chem. Phys., 14, 8521–8531, doi:10.5194/acp-14-8521-2014, 2014.

Tobo, Y., Prenni, A. J., DeMott, P. J., Huffman, J. A., McCluskey, C. S., Tian, G., Pöhlker, C., Pöschl, U. and Kreidenweis, S. M.: Biological aerosol particles as a key determinant of ice nuclei populations in a forest ecosystem, J. Geophys. Res.-Atmos., 118, 10100–10110, doi:10.1002/jgrd.50801, 2013.

Tsumuki, H., Konno, H., Maeda, T. and Okamoto, Y.: An ice-nucleating active fungus isolated from the gut of the rice stem borer, *Chilo suppressalis* Walker (Lepidoptera: Pyralidae), J. Insect Physiol., 38, 119–125, doi:10.1016/0022-1910(92)90040-K, 1992.

Twohy, C. H., DeMott, P. J., Pratt, K. A., Subramanian, R., Kok, G. L., Murphy, S. M., Lersch, T., Heymsfield, A. J., Wang, Z., Prather, K. A. and Seinfeld, J. H.: Relationships of Biomass-Burning Aerosols to Ice in Orographic Wave Clouds, J. Atmos. Sci., 67, 2437–2450, doi:10.1175/2010JAS3310.1, 2010.

United States Environmental Protection Agency, Air Emission Sources, http://www.epa.gov/air/emissions/index.htm (last access: 7 April 2015), 2014.

Vali, G.: Quantitative Evaluation of Experimental Results on the Heterogeneous Freezing Nucleation of Supercooled Liquids, J. Atmos. Sci., 28, 402–409, 1971.

Vali, G.: Nucleation Terminology, J. Aerosol Sci., 16, 575–576, doi:10.1016/0021-8502(85)90009-6, 1985.

Vali, G., DeMott, P. J., Möhler, O. and Whale, T. F.: Technical Note: A proposal for ice nucleation terminology, Atmos. Chem. Phys., 15, 10263–10270, doi:10.5194/acp-15-10263-2015, 2015.

von Blohn, N., Mitra, S. K., Diehl, K. and Borrmann, S.: The ice nucleating ability of pollen: Part III. New laboratory studies in immersion and contact freezing modes including more pollen types, Atmos. Res., 78, 182–189, doi:10.1016/j.atmosres.2005.03.008, 2005.

Webster, J. and Weber, R. W. S.: Introduction to Fungi, Third Edition, Cambridge University Press, New York, NY, USA, 2007.

Welti, A., Lüönd, F., Kanji, Z. A., Stetzer, O. and Lohmann, U.: Time dependence of immersion freezing: an experimental study on size selected kaolinite particles, Atmos. Chem. Phys., 12, 9893–9907, doi:10.5194/acp-12-9893-2012, 2012.

Wheeler, M. J. and Bertram, A. K.: Deposition nucleation on mineral dust particles: a case against classical nucleation theory with the assumption of a single contact angle, Atmos. Chem. Phys., 12, 1189–1201, doi:10.5194/acp-12-1189-2012, 2012.

Wheeler, M. J., Mason, R. H., Steunenberg, K., Wagstaff, M., Chou, C. and Bertram, A. K.: Immersion Freezing of Supermicron Mineral Dust Particles: Freezing Results, Testing Different Schemes for Describing Ice Nucleation, and Ice Nucleation Active Site Densities, J. Phys. Chem. A, 119, 4358–4372, doi:10.1021/jp507875q, 2015.

Whitney, F. A., Crawford, W. R. and Harrison, P. J.: Physical processes that enhance nutrient transport and primary productivity in the coastal and open ocean of the subarctic NE Pacific, Deep Sea Res. Part II Top. Stud. Oceanogr., 52, 681–706, doi:10.1016/j.dsr2.2004.12.023, 2005.

Wilson, T. W., Ladino, L. A., Alpert, P. A., Breckels, M. N., Brooks, I. M., Browse, J., Burrows, S. M., Carslaw, K. S., Huffman, J. A., Judd, C., Kilthau, W. P., Mason, R. H., McFiggans, G., Miller, L. A., Nájera, J. J., Polishchuk, E., Rae, S., Schiller, C. L., Si, M., Vergara Temprado, J., Whale, T. F., Wong, J. P. S., Wurl, O., Yakobi-Hancock, J. D., Abbatt, J. P. D., Aller, J. Y., Bertram, A. K., Knopf, D. A. and Murray, B. J.: A marine biogenic source of atmospheric ice nucleating particles, Nature, 525, 234–238, doi:10.1038/nature14986, 2015.

Wright, T. P. and Petters, M. D.: The role of time in heterogeneous freezing nucleation, J. Geophys. Res.-Atmos., 118, 3731–3743, doi:10.1002/jgrd.50365, 2013.

Wright, T. P., Petters, M. D., Hader, J. D., Morton, T. and Holder, A. L.: Minimal cooling rate dependence of ice nuclei activity in the immersion mode, J. Geophys. Res.-Atmos., 118, 10535–10543, doi:10.1002/jgrd.50810, 2013.

Yakobi-Hancock, J. D., Ladino, L. A. and Abbatt, J. P. D.: Feldspar minerals as efficient deposition ice nuclei, Atmos. Chem. Phys., 13, 11175–11185, doi:10.5194/acp-13-11175-2013, 2013.

Yakobi-Hancock, J. D., Ladino, L. A., Bertram, A. K., Huffman, J. A., Jones, K., Leaitch, W. R., Mason, R. H., Schiller, C. L., Toom-Sauntry, D., Wong, J. P. S. and Abbatt, J. P. D.: CCN activity of size-selected aerosol at a Pacific coastal location, Atmos. Chem. Phys., 14, 12307–12317, doi:10.5194/acp-14-12307-2014, 2014.

Yang, M., Howell, S. G., Zhuang, J. and Huebert, B. J.: Attribution of aerosol light absorption to black carbon, brown carbon, and dust in China - interpretations of atmospheric measurements during EAST-AIRE, Atmos. Chem. Phys., 9, 2035–2050, doi:10.5194/acp-9-2035-2009, 2009.

Yun, Y. and Penner, J. E.: An evaluation of the potential radiative forcing and climatic impact of marine organic aerosols as heterogeneous ice nuclei, Geophys. Res. Lett., 40, 4121–4126, doi:10.1002/grl.50794, 2013.

Zimmermann, F., Weinbruch, S., Schütz, L., Hofmann, H., Ebert, M., Kandler, K. and Worringen, A.: Ice nucleation properties of the most abundant mineral dust phases, J. Geophys. Res., 113, D23204, doi:10.1029/2008JD010655, 2008.

**Table 1.** Correlation coefficients ($R$) for linear regression analyses of INPs versus fluorescent bioparticles, total aerosol particles, eBC, sodium, MSA, and wind speed[a]. Correlations with statistical significance ($P < 0.05$) are shown in bold.

| | Relation to the INP number concentration | | | | | | | | | | | |
|---|---|---|---|---|---|---|---|---|---|---|---|---|
| | -15 °C | | | -20 °C | | | -25 °C | | | -30 °C | | |
| Measurement | *R* | *P*[b] | *n*[c] | *R* | *P* | *n* | *R* | *P* | *n* | *R* | *P* | *n* |
| Fluorescent bioparticles [0.5–10 µm] | **0.74** | < 0.01 | 28 | **0.77** | < 0.01 | 28 | **0.83** | < 0.01 | 28 | **0.66** | < 0.01 | 23 |
| Total particles [0.5–10 µm] | **0.33** | 0.04 | 28 | **0.36** | 0.03 | 28 | **0.49** | < 0.01 | 28 | **0.66** | < 0.01 | 23 |
| eBC | **0.47** | < 0.01 | 34 | **0.59** | < 0.01 | 34 | **0.60** | < 0.01 | 34 | 0.25 | 0.11 | 27 |
| Sodium | -0.35 | 0.25 | 6 | 0.13 | 0.40 | 6 | 0.32 | 0.27 | 6 | 0.82 | 0.20 | 3 |
| MSA | 0.17 | 0.38 | 6 | 0.51 | 0.15 | 6 | 0.27 | 0.30 | 6 | 0.00 | 0.50 | 3 |
| $(\text{Wind speed})^{3.41}$ [lighthouse] | 0.05 | 0.39 | 34 | 0.01 | 0.48 | 34 | 0.15 | 0.19 | 34 | **0.48** | < 0.01 | 27 |
| $(\text{Wind speed})^{3.41}$ [buoy] | 0.04 | 0.40 | 34 | 0.04 | 0.40 | 34 | 0.19 | 0.14 | 34 | **0.55** | < 0.01 | 27 |

[a]Using the power law dependence of whitecap coverage on wind speed found by Monahan and Muircheartaigh (1980), wind speed was raised to the power of 3.41.
[b]The $P$ value is a conditional probability that is the probability of obtaining an $R$ value equal to or greater than the given $R$ value if there is no correlation between INPs and the given parameter.
[c]$n$ represents the number of data points used in determining the correlation.

**Table 2.** Correlation coefficients ($R$) for linear regression analyses of INPs versus fluorescent bioparticles, total aerosol particles, eBC, and wind speed[a] within each category of air mass. Correlations with statistical significance ($P < 0.05$) are shown in bold.

| | | Relation to the INP number concentration | | | | | | | | | | | |
|---|---|---|---|---|---|---|---|---|---|---|---|---|---|
| | | -15 °C | | | -20 °C | | | -25 °C | | | -30 °C | | |
| Air Mass | Measurement | *R* | *P*[b] | *n*[c] | *R* | *P* | *n* | *R* | *P* | *n* | *R* | *P* | *n* |
| Coastal NW | Fluorescent bioparticles [0.5–10 µm] | **0.94** | <0.01 | 9 | **0.94** | <0.01 | 9 | **0.96** | <0.01 | 9 | 0.65 | 0.08 | 6 |
| | Total particles [0.5–10 µm] | **0.85** | <0.01 | 9 | **0.70** | 0.02 | 9 | **0.71** | 0.02 | 9 | 0.67 | 0.07 | 6 |
| | eBC | **0.71** | <0.01 | 11 | **0.80** | <0.01 | 11 | **0.84** | <0.01 | 11 | 0.53 | 0.11 | 7 |
| | (Wind speed)$^{3.41}$ [lighthouse] | -0.38 | 0.12 | 11 | -0.39 | 0.12 | 11 | -0.22 | 0.26 | 11 | 0.26 | 0.29 | 7 |
| | (Wind speed)$^{3.41}$ [buoy] | -0.03 | 0.47 | 11 | 0.00 | 0.49 | 11 | 0.00 | 0.50 | 11 | -0.02 | 0.48 | 7 |
| Coastal SE | Fluorescent bioparticles [0.5–10 µm] | -0.07 | 0.48 | 3 | -0.53 | 0.32 | 3 | -0.85 | 0.17 | 3 | NA[d] | | |
| | Total particles [0.5–10 µm] | -0.17 | 0.45 | 3 | -0.61 | 0.29 | 3 | -0.90 | 0.14 | 3 | NA | | |
| | eBC | 0.07 | 0.46 | 5 | 0.28 | 0.32 | 5 | 0.67 | 0.11 | 5 | 0.96 | 0.09 | 3 |
| | (Wind speed)$^{3.41}$ [lighthouse] | -0.34 | 0.29 | 5 | -0.27 | 0.33 | 5 | -0.14 | 0.41 | 5 | 0.21 | 0.43 | 3 |
| | (Wind speed)$^{3.41}$ [buoy] | -0.52 | 0.18 | 5 | -0.37 | 0.27 | 5 | -0.12 | 0.43 | 5 | 0.93 | 0.12 | 3 |
| Pacific Ocean | Fluorescent bioparticles [0.5–10 µm] | **0.80** | <0.01 | 12 | **0.74** | <0.01 | 12 | **0.64** | 0.01 | 12 | 0.23 | 0.24 | 12 |
| | Total particles [0.5–10 µm] | 0.13 | 0.34 | 12 | 0.30 | 0.17 | 12 | 0.21 | 0.25 | 12 | 0.25 | 0.22 | 12 |
| | eBC | 0.24 | 0.21 | 14 | 0.37 | 0.10 | 14 | 0.26 | 0.19 | 14 | 0.06 | 0.42 | 13 |
| | (Wind speed)$^{3.41}$ [lighthouse] | -0.10 | 0.37 | 14 | -0.26 | 0.18 | 14 | -0.26 | 0.19 | 14 | -0.21 | 0.25 | 13 |
| | (Wind speed)$^{3.41}$ [buoy] | -0.18 | 0.27 | 14 | -0.38 | 0.09 | 14 | **-0.48** | 0.04 | 14 | -0.22 | 0.23 | 13 |
| Free troposphere | Fluorescent bioparticles [0.5–10 µm] | **0.97** | 0.02 | 4 | **0.99** | <0.01 | 4 | **0.99** | <0.01 | 4 | **1.00** | <0.01 | 4 |
| | Total particles [0.5–10 µm] | 0.86 | 0.07 | 4 | **0.98** | 0.01 | 4 | **0.99** | <0.01 | 4 | **0.98** | 0.01 | 4 |
| | eBC | **0.99** | <0.01 | 4 | 0.89 | 0.05 | 4 | 0.88 | 0.06 | 4 | 0.89 | 0.06 | 4 |
| | (Wind speed)$^{3.41}$ [lighthouse] | -0.89 | 0.05 | 4 | -0.70 | 0.15 | 4 | -0.67 | 0.17 | 4 | -0.68 | 0.16 | 4 |
| | (Wind speed)$^{3.41}$ [buoy] | 0.62 | 0.19 | 4 | 0.39 | 0.31 | 4 | 0.38 | 0.31 | 4 | 0.42 | 0.29 | 4 |

[a]Using the power law dependence of whitecap coverage on wind speed found by Monahan and Muircheartaigh (1980), wind speed was raised to the power of 3.41.
[b]The $P$ value is a conditional probability that is the probability of obtaining an $R$ value equal to or greater than the given $R$ value if there is no correlation between INPs and the given parameter.
[c]$n$ represents the number of data points used in determining the correlation.
[d]NA = not available due to insufficient data.

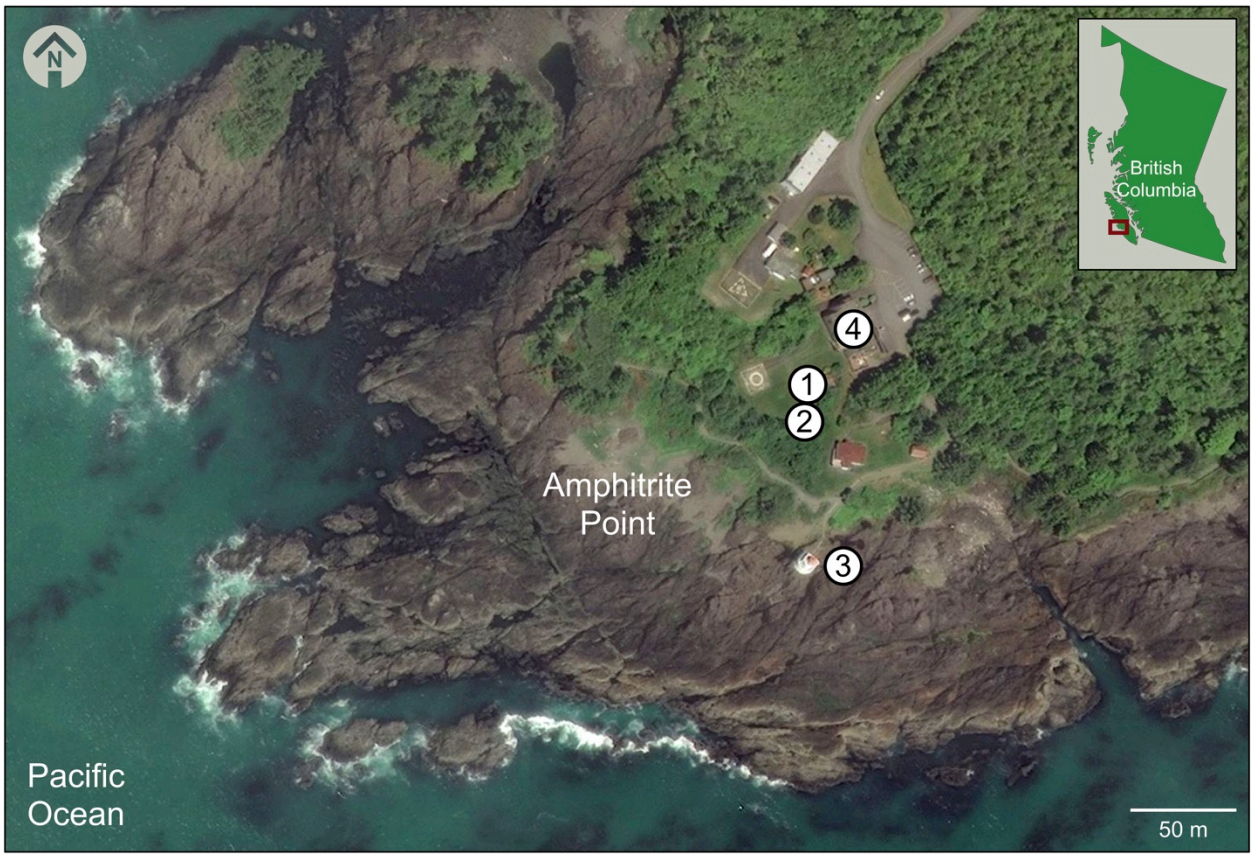


**Figure 1.** A satellite image of the sampling site: (1) location of the MOUDIs and the WIBS-4A; (2) location of the MAAP; (3) Amphitrite Lighthouse where most meteorological data was collected; and (4) a station of the Canadian Coast Guard with supporting infrastructure. The image was modified from Bing Maps, 2014 (http://www.bing.com/maps/). Inset: the location of the sampling site in British Columbia, Canada.

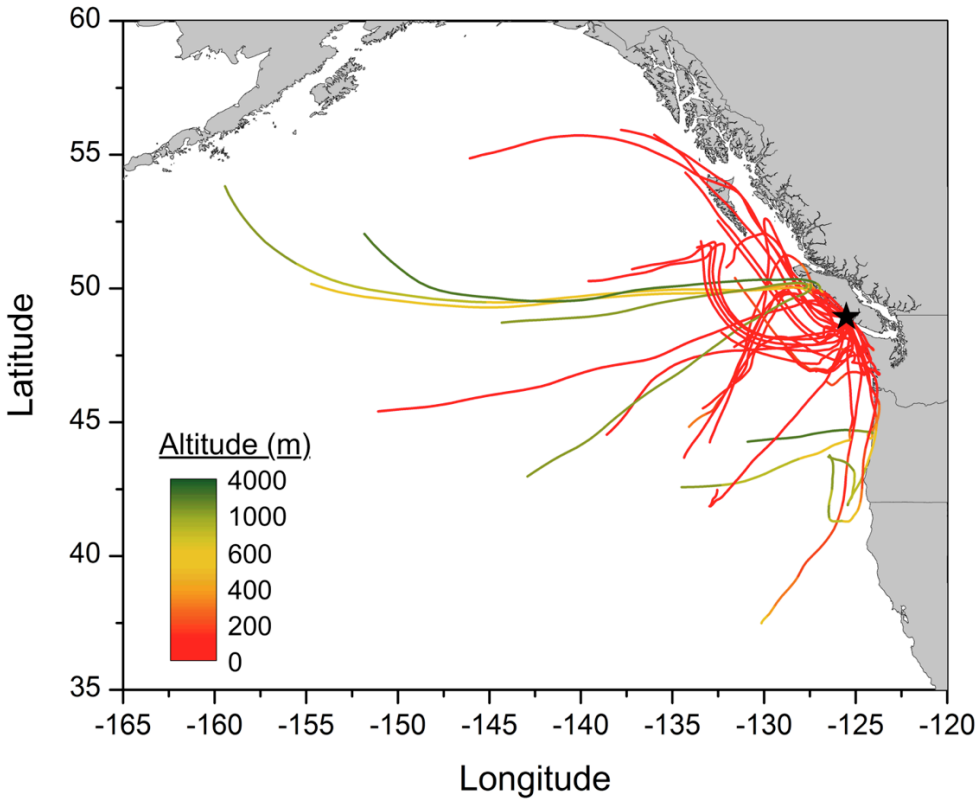


**Figure 2.** Seventy-two hour HYSPLIT4 back trajectories of the air masses analyzed at the coastal site (black star) during INP sampling periods. Each back trajectory was initiated from a height of 5.5 m agl and at the midpoint of the sampling period.

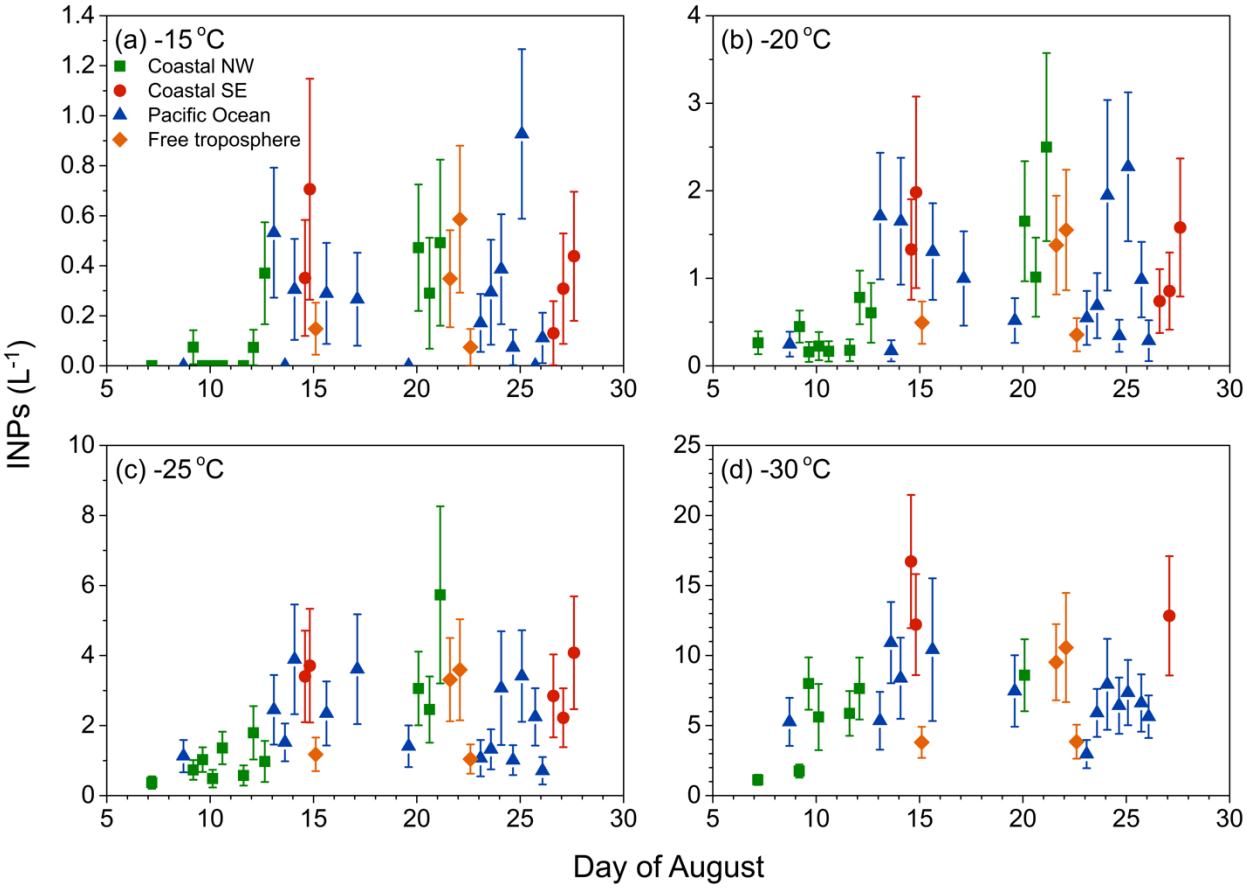


**Figure 3.** INP number concentrations as a function of date determined at ice-activation temperatures of (a) -15 °C, (b) -20 °C, (c) -25 °C, and (d) -30 °C. The symbols are color coded by air mass category (see Sect. 2.8 for details). Fewer data points are available at -30 °C as INP number concentrations can only be determined to the temperature where all droplets are frozen and Eq. (1) becomes undefined.

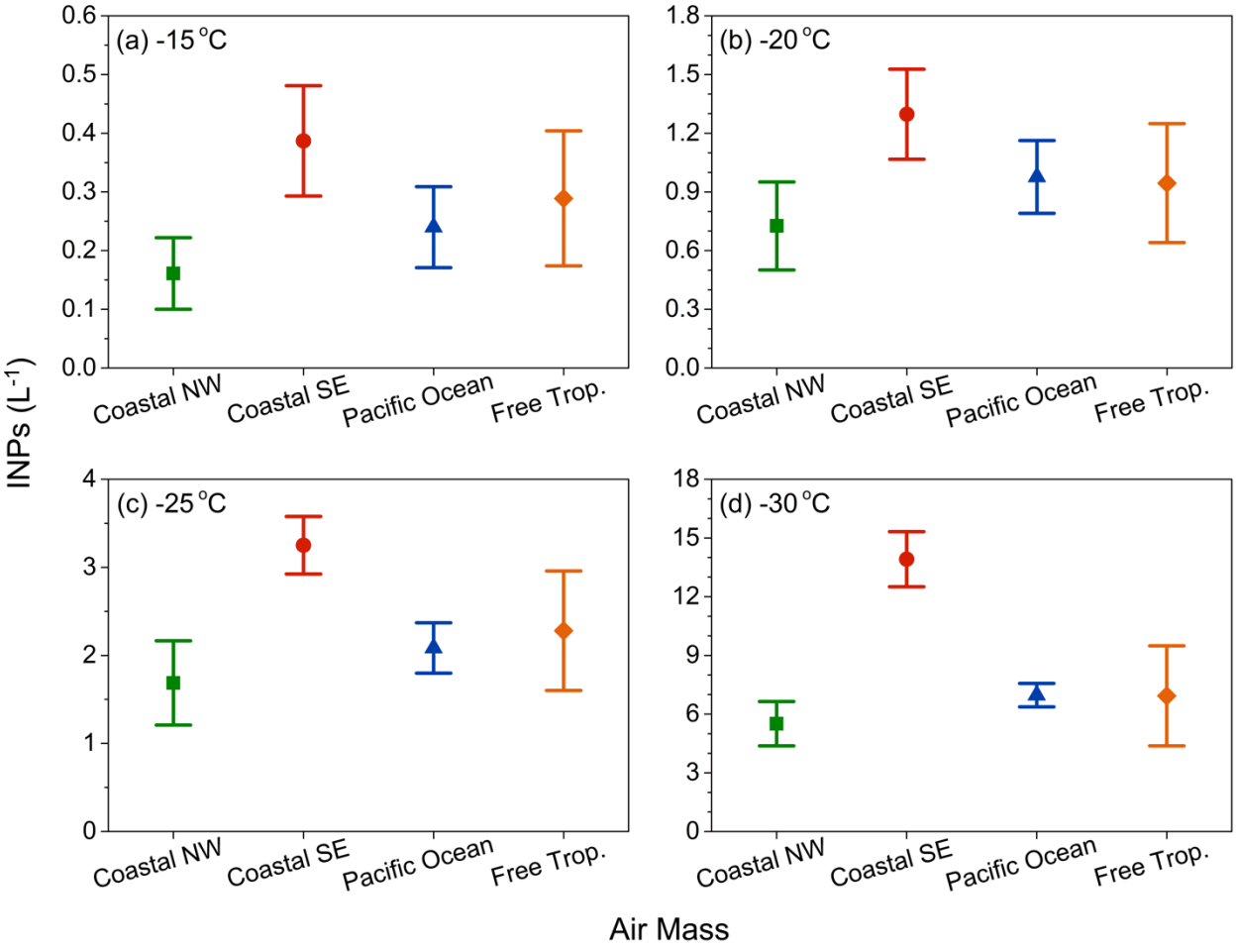


**Figure 4.** Mean INP number concentrations found in each of the four categories of air masses sampled at (a) -15 °C, (b) -20 °C, (c) -25 °C, and (d) -30 °C. The scheme for air mass classification is given in Sect. 2.8. Uncertainties are given as the standard error of the mean.

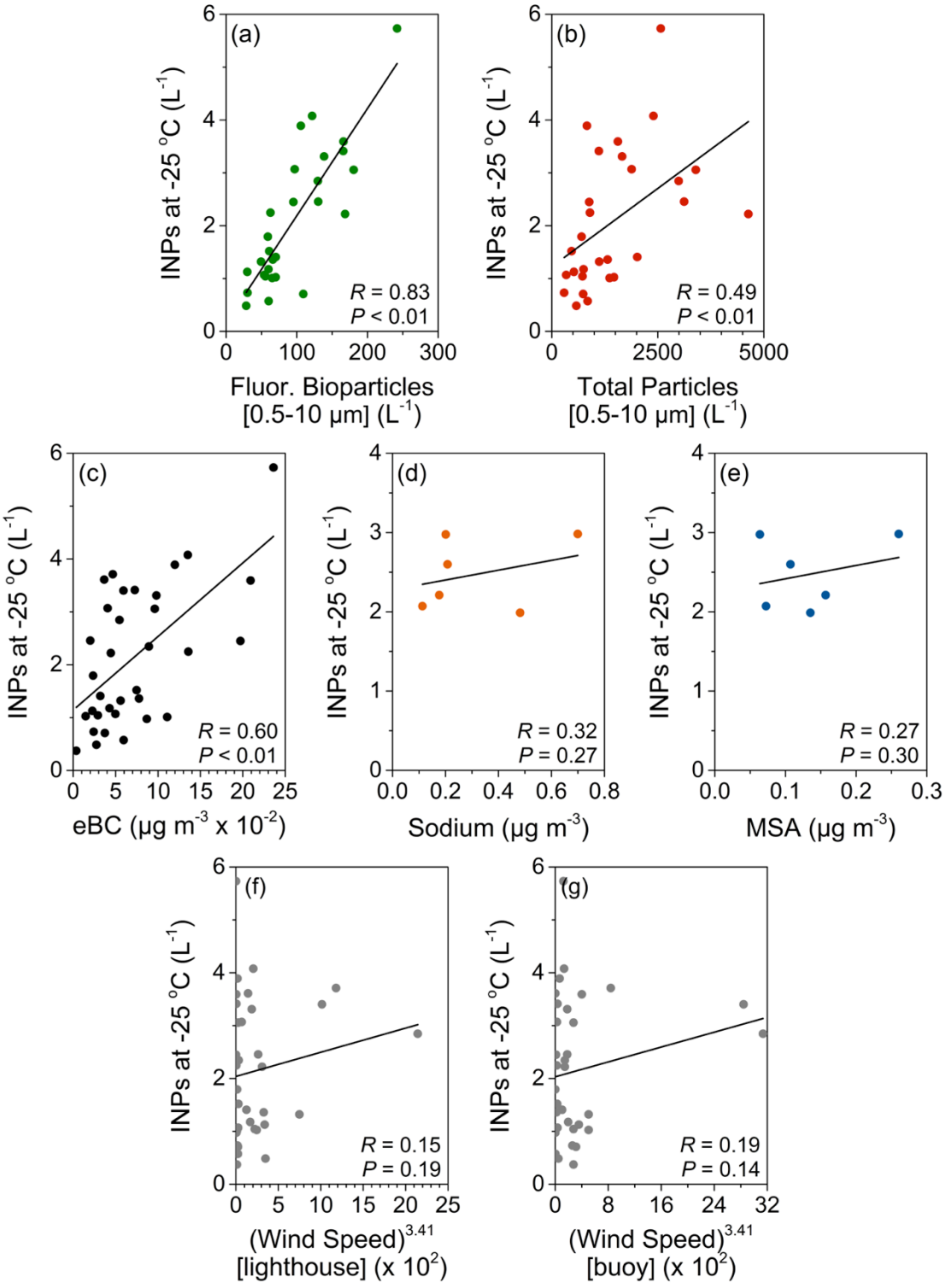


**Figure 5.** Number concentrations of INPs active at -25 °C plotted against concentrations of (a) fluorescent bioparticles 0.5–10 µm, (b) total particles 0.5–10 µm, (c) eBC, (d) sodium, (e) MSA, and (f–g) (wind speed)$^{3.41}$ based on the power law function of Monahan and Muircheartaigh (1980) where wind speed was in units of m s$^{-1}$. Linear fits are shown with corresponding correlation coefficients ($R$) and probability values ($P$).

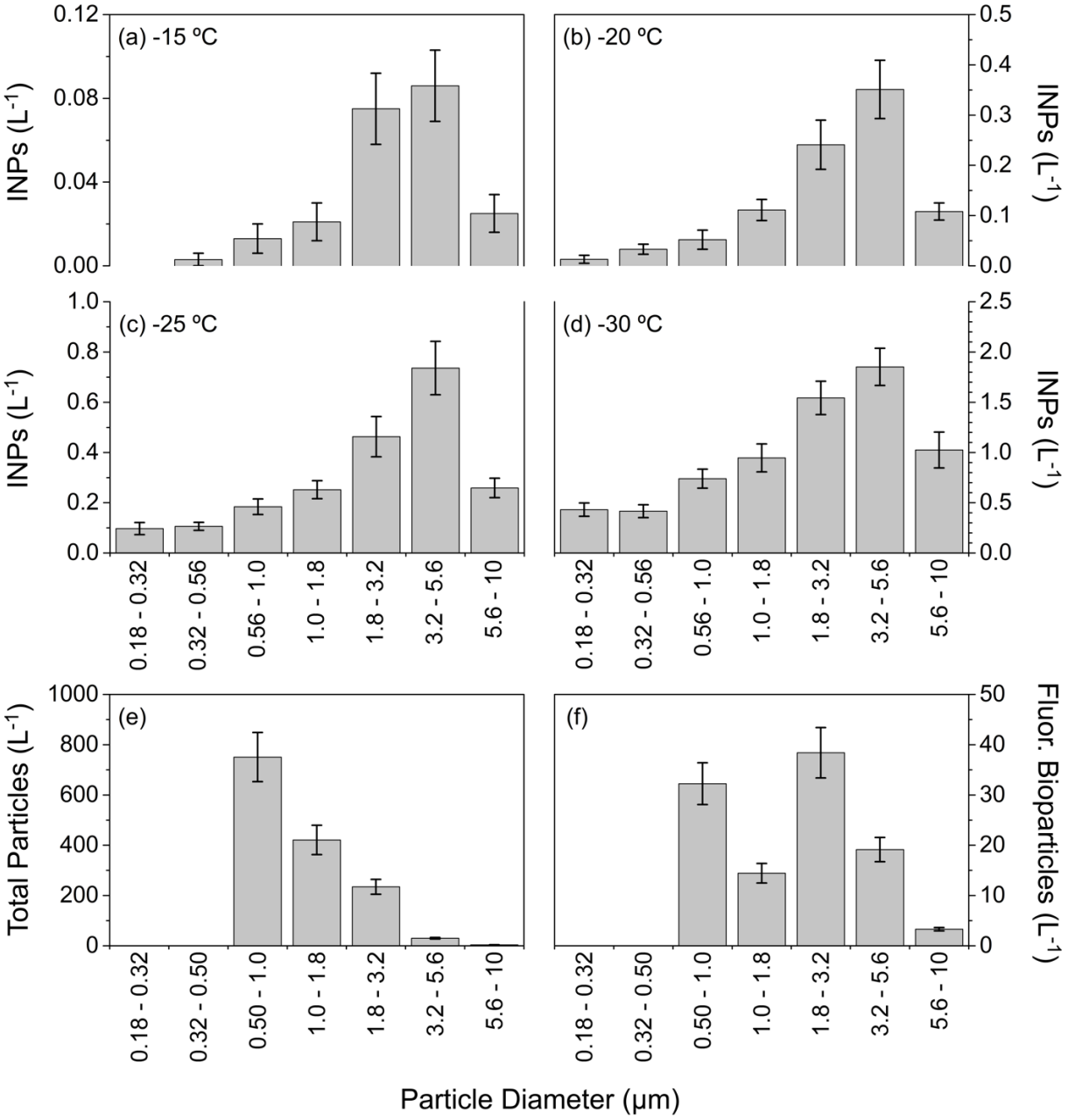


**Figure 6.** Mean number concentrations as a function of size for INPs active at (a) -15 °C, (b) -20 °C, (c) -25 °C, and (d) -30 °C, total particles (e) and fluorescent bioparticles (f) using only samples where both the MOUDI-DFT and WIBS-4A were operating. Uncertainties are given as the standard error of the mean. As INP number concentrations can only be determined at temperatures less than the temperature where all droplets are frozen and Eq. (1) becomes undefined, fewer samples are represented at -30 °C. Number concentrations below 0.5 µm were not measured by the WIBS-4A for panels (e) and (f) but plot axes are consistent for easier comparison of the size distributions.

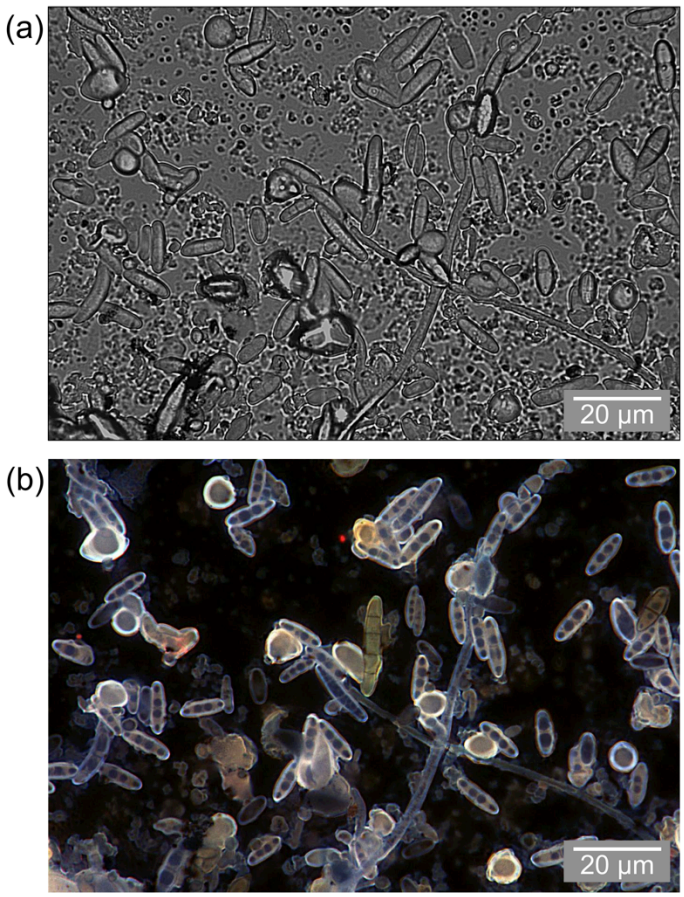


**Figure 7.** Fluorescence microscopy images of an aerosol sample collected on August 11, 2013: (a) bright-field image; (b) an overlay of red, green, and blue fluorescence channels. A blue coloration is characteristic of biological material (Pöhlker et al., 2012).

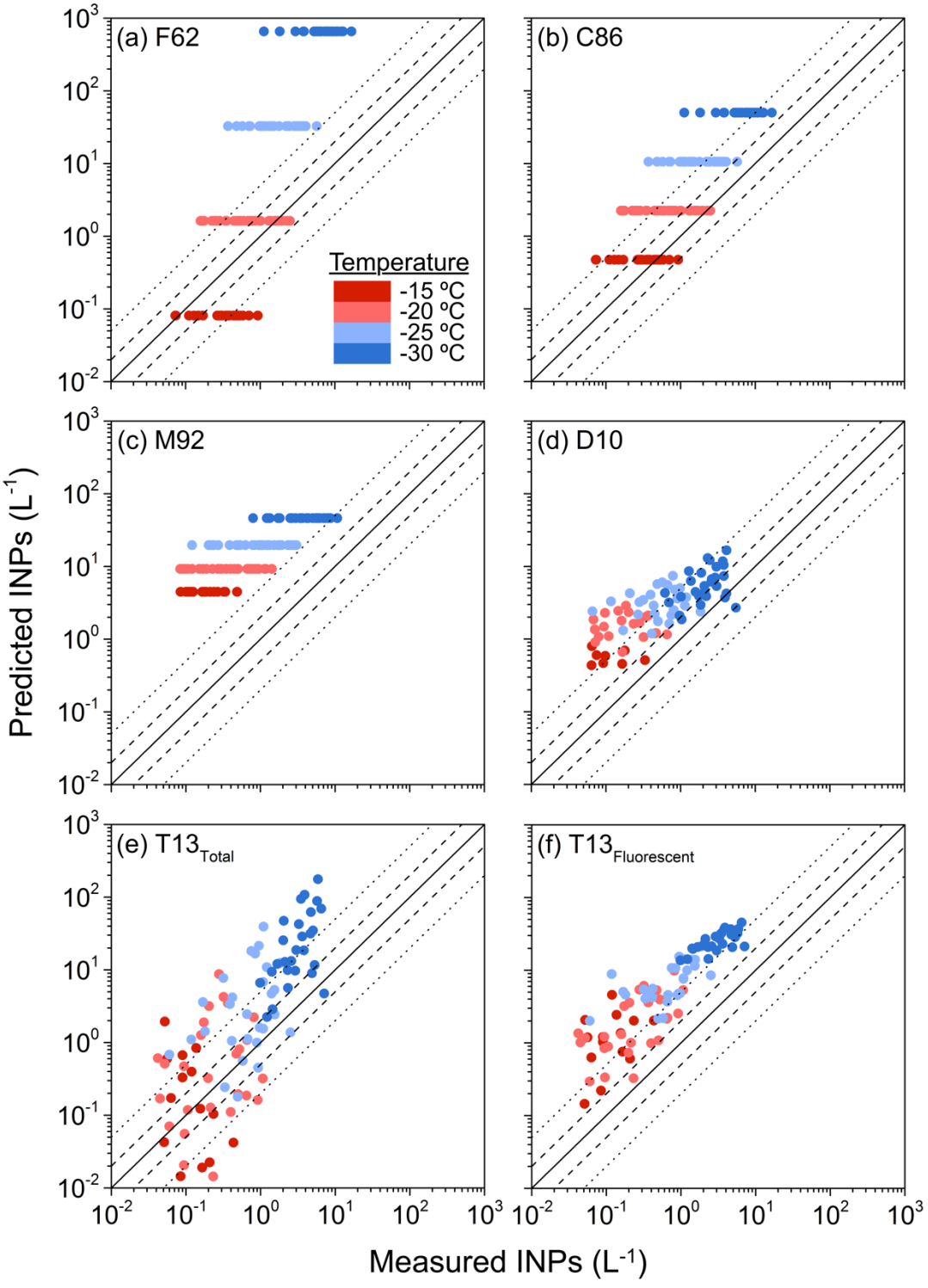


**Figure 8.** Predicted versus measured INP number concentrations based on the parameterizations of (a) Fletcher (1962); (b) Cooper (1986); (c) Meyers et al. (1992); (d) DeMott et al. (2010); and (e–f) Tobo et al. (2013). Details on these parameterizations are given in the Supplement. Data color represents ice nucleation temperatures. This figure uses the format of Fig. 9 in Tobo et al. (2013).